



DUDLEY KNOX LIBRARY
NAVAL POC
MONTEREY, CALIFORNIA 93943

NAVAL POSTGRADUATE SCHOOL

Monterey, California



THESIS

CERENKOV RADIATION FROM PERIODIC BUNCHES
FOR A FINITE PATH IN AIR

by

Robert George Bruce

June 1985

Thesis Advisor
Co-Advisor

Xavier K. Maruyama
J. R. Neighbours

Approved for Public Release: distribution is unlimited

T222796

SECURITY CLASSIFICATION OF THIS PAGE (When Data Entered)

REPORT DOCUMENTATION PAGE		READ INSTRUCTIONS BEFORE COMPLETING FORM
1. REPORT NUMBER	2. GOVT ACCESSION NO.	3. RECIPIENT'S CATALOG NUMBER
4. TITLE (and Subtitle) Cerenkov Radiation from Periodic Bunches for a Finite Beam Path in Air		5. TYPE OF REPORT & PERIOD COVERED Masters Thesis June 1985
7. AUTHOR(s) Robert G. Bruce, CDR, USN		6. PERFORMING ORG. REPORT NUMBER
9. PERFORMING ORGANIZATION NAME AND ADDRESS Naval Postgraduate School Monterey, California 93943-5100		8. CONTRACT OR GRANT NUMBER(s)
11. CONTROLLING OFFICE NAME AND ADDRESS Naval Postgraduate School Monterey, California 93943-5100		10. PROGRAM ELEMENT, PROJECT, TASK AREA & WORK UNIT NUMBERS
14. MONITORING AGENCY NAME & ADDRESS (if different from Controlling Office)		12. REPORT DATE June 1985
		13. NUMBER OF PAGES 80
		15. SECURITY CLASS. (of this report) Unclassified
16. DISTRIBUTION STATEMENT (of this Report) Approved for public release; distribution unlimited		15a. DECLASSIFICATION/DOWNGRADING SCHEDULE
17. DISTRIBUTION STATEMENT (of the abstract entered in Block 20, if different from Report)		
18. SUPPLEMENTARY NOTES		
19. KEY WORDS (Continue on reverse side if necessary and identify by block number) Cerenkov Radiation Periodic electron bunches Diffraction Pattern		
20. ABSTRACT (Continue on reverse side if necessary and identify by block number) The equation as derived by F. R. Buskirk and J. R. Neighbours for the power in the diffraction pattern of Cerenkov radiation from periodic bunches in air is experimentally tested at the Naval Postgraduate School Accelerator Laboratory (NPSAL). Previous experiments done at NPSAL are briefly reviewed. the experiment focuses on reducing RF noise and introduces a method for recording experimental data. RF noise is divided into two		

categories: 1) Noise received directly at the antenna, and 2) noise picked up by the cabling. Category 1 is divided into two subcategories: a) Cerenkov radiation received by the antenna after being reflected off secondary objects, and b) residual klystron radiation. Experimental data curves from the third harmonic are compared to theoretical patterns for various finite emission lengths and angle shifts. The data demonstrates that noise-generated fine structure which appeared in a previous experiment at NPSAL can be eliminated with increased shielding.

Approved for public release; distribution unlimited

Cerenkov Radiation from Periodic Bunches
for a Finite Beam Path in Air

by

Robert G. Bruce
Commander, United States Navy
B.A. University of California, 1967

Submitted in partial fulfillment of the
requirements for the degree of

MASTER OF SCIENCE IN PHYSICS

from the

NAVAL POSTGRADUATE SCHOOL
June 1985

1963
2527
7.1

ABSTRACT

The equation as derived by F. R. Buskirk and J. R. Neighbours for the power in the diffraction pattern of Cerenkov radiation from periodic bunches in air is experimentally tested at the Naval Postgraduate School Accelerator Laboratory (NPSAL). Previous experiments done at NPSAL are briefly reviewed. The experiment focuses on reducing RF noise and introduces a method for recording experimental data. RF noise is divided into two categories: 1) Noise received directly at the antenna, and 2) noise picked up by the cabling. Category 1 is divided into two subcategories: a) Cerenkov radiation received by the antenna after being reflected off secondary objects, and b) residual klystron radiation. Experimental data curves from the third harmonic are compared to theoretical patterns for various finite emission lengths and angle shifts. The data demonstrates that noise-generated fine structure which appeared in a previous experiment at NPSAL can be eliminated with increased shielding.

TABLE OF CONTENTS

I.	INTRODUCTION.....	7
A.	BACKGROUND.....	7
B.	PREVIOUS EXPERIMENTS.....	20
C.	PURPOSE.....	24
II.	THE EXPERIMENT.....	26
A.	EXPERIMENTAL SETUP.....	26
B.	NOISE REDUCTION.....	32
C.	COLLECTING DATA.....	42
III.	RESULTS AND CONCLUSIONS.....	47
A.	RESULTS.....	47
B.	CONCLUSIONS.....	57
APPENDIX A:	DESCRIPTION OF EQUIPMENT.....	67
APPENDIX B:	SUGGESTIONS FOR FUTURE WORK.....	72
APPENDIX C:	TABULATED DATA FROM FIGURES 24, 25, 26, AND 27.....	73
LIST OF REFERENCES.....		79
INITIAL DISTRIBUTION LIST.....		80

ACKNOWLEDGEMENTS

I wish to thank my thesis advisors, Professors X. K. Maruyama, who graciously tolerated much more than he should have, and J. R. Neighbours, whose earlier work inspired this experiment, for their guidance, assistance, and instruction. I also want to thank Don Snyder for his assistance in the design of the experimental setup.

Finally, I am grateful to my wife, Penny, who helped in the organization of the paper and spent many hours proofing and editing the final draft.

This paper is dedicated to my children, Bethy and Robby.

I. INTRODUCTION

A. BACKGROUND

Cerenkov radiation is commonly known as the pale blue light emitted from a transparent medium that surrounds a source of high radioactivity. Cerenkov radiation occurs when a charged particle moves through a transparent medium at a velocity that is greater than the velocity of light in the medium. As the charged particle passes through the medium the atoms become polarized and set up a polarized field asymmetrical in the direction of the particle's motion. The asymmetrical field causes radiation to be emitted at an angle to the direction of the particle such that the "Cerenkov relation" is satisfied:

$$\cos \theta_c = \frac{c'}{v}$$

where

$$c' = \frac{c}{n}$$

and n is the refractive index of the medium and c is the speed of light in a vacuum.

Assume that the radiation is observed at infinity and that the particle's path is infinite in length. The radiated power of the Cerenkov phenomenon can then be calculated after deriving the E and H fields from the wave

equations for the scalar and vector potentials generated by the current and charge densities of the particle [Ref. 1]. This results in an equation for the radiation through the surface of a cylinder of length l (Equation 2.17, [Ref. 1]) representing infinite spectra and, therefore, producing infinite radiation output.

$$\frac{dW}{d\omega dl} = \frac{e^2}{c^2} \int_{\beta n > 1} \left(1 - \frac{1}{\beta^2 n^2}\right) \omega d\omega$$

In reality, however, all media are dispersive, and absorption bands exist throughout the spectrum, bringing the radiation to finite levels [Ref. 1]. For small portions of the spectrum, media can be considered dispersionless.

The radiation is coherent only at the angle Θ_C because in an increment of time (Δt) the particle will move a certain distance ($v\Delta t$) while the radiation field moves a smaller distance ($c'\Delta t$). The radiation moves away from the area of the particle in a manner similar to the wake of a ship. Huygen's principle explains the coherency of the wave front [Ref. 1]. Since the particle travels through a three dimensional medium, the wave front takes a conical shape (Figure 1).

The pale blue light was observed by Madame Curie in 1910 with samples of radium. The first experimental work on the phenomenon was reported in 1926 by L. Mallet and then in 1934 by P. A. Cerenkov who continued his investigations

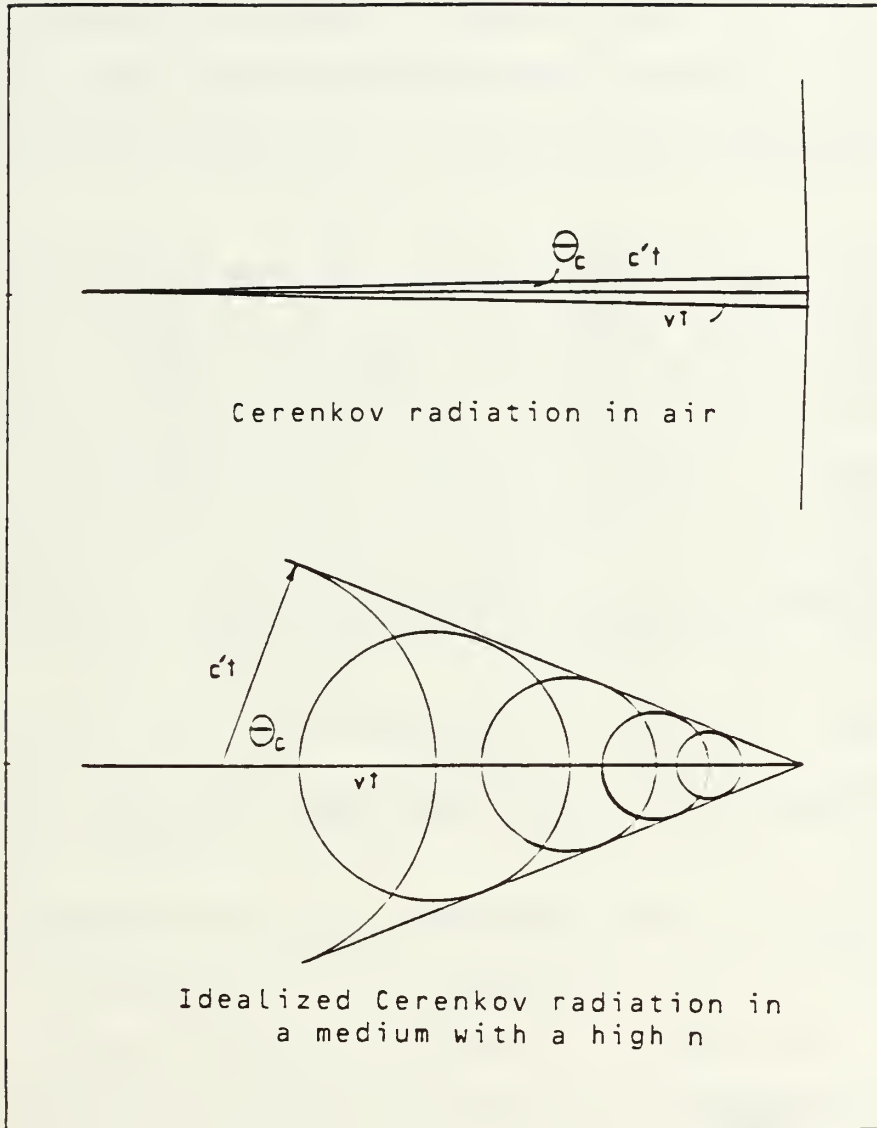


Figure 1 Cerenkov Radiation

until 1938. In 1937 a classical explanation for the radiation was proposed by I. M. Frank and I. Tamm. In 1940 V. L. Ginsburg advanced a quantum theory for the radiation. From then on it was known as Cerenkov radiation. A theoretical treatment and compendium of research done on Cerenkov radiation was done by J. V. Jelley in 1958. [Ref. 1]

Buskirk and Neighbours [Ref. 2], working at the Naval Postgraduate School Accelerator Laboratory (NPSAL) in 1982, formulated the equation for the power of Cerenkov radiation from periodic bunches of electrons in a medium of finite interaction length. The equation also predicted the power from the harmonics of the fundamental period. Buskirk and Neighbors expanded their study in 1983 [Ref. 3] to include the diffraction effects in the radiation. The relation for the diffracted power radiated in watts per steradian is given by:

$$W(\nu, \hat{n}) = \nu_0^2 Q R^2 \text{ (watts/steradian)} \quad \text{(Equation 1)}$$

where

$$Q = \frac{4c}{8\pi} q^2$$

q = charge in electron bunch

ν_0 = frequency of the linac (2.86 GHz)

$$R = kL \sin\Theta I(u)F(\vec{k})$$

and where

$$k = \frac{2\pi}{\lambda} = \text{wave number of Cerenkov radiation} \\ = jk_0 \quad (k_0 = \text{wave number for } \nu_0), \quad j = \text{integer}$$

L = finite interaction beam length

$$u = \frac{kL}{2} (\cos \Theta_C - \cos \Theta)$$

$$I(u) = \frac{\sin u}{u} = \text{diffraction pattern}$$

$F(\bar{k})$ = form factor of the charge distribution bunch

The equation assumes that the observer is in the far field and says that the radiated power is dependent on the angle to the beam according to the diffraction function (I). Turner did experimental work on the effects of the form factor ($F(\bar{k})$) at NPSAL in 1984 [Ref. 4]. In the present experiment, where the bunch length is small compared to the wavelength, the form factor can be considered unity.

TABLE 1

NPS ACCELERATOR LABORATORY (NPSAL) CHARACTERISTICS

Beam Energy	100 MeV	
Bunch Period	2.856E9 Hz	
Bunch Length	0.0024 m	[Ref. 4]
Bunch Distance	0.103 m	[Ref. 4]
Bunch Charge	1.16E-12 C	[Ref. 5]

If the characteristics of Table 1 were applied to Equation 1 then the finite beam interaction length (L) would

have to be kept small. The limiting factor to L for a given harmonic of the fundamental frequency is the distance to the far field (r), where r is determined by the dimensions of the experiment station illustrated in Figure 2. Table 2 shows the distance to the far field for several finite interaction lengths (L) in the third and fourth harmonics with values calculated from the relation [Ref. 6]:

$$r = \frac{2L^2}{\lambda}$$

In this relation, λ is the wavelength of the particular harmonic of interest.

TABLE 2
DISTANCE TO THE FAR FIELD

L(meters)	Third Harmonic	Fourth Harmonic
	r(meters)	r(meters)
0.05	0.14	0.19
0.10	0.57	0.76
0.13	0.96	1.28
0.15	1.28	1.71
0.16	1.46	1.94
0.20	2.28	3.05

The diffraction patterns, solved from Equation 1, for several of these parameters and the characteristics from Table 1 are shown in Figures 3 through 7.

Can Equation 1, representing the power of a phenomenon akin to the pale blue light, be experimentally verified at

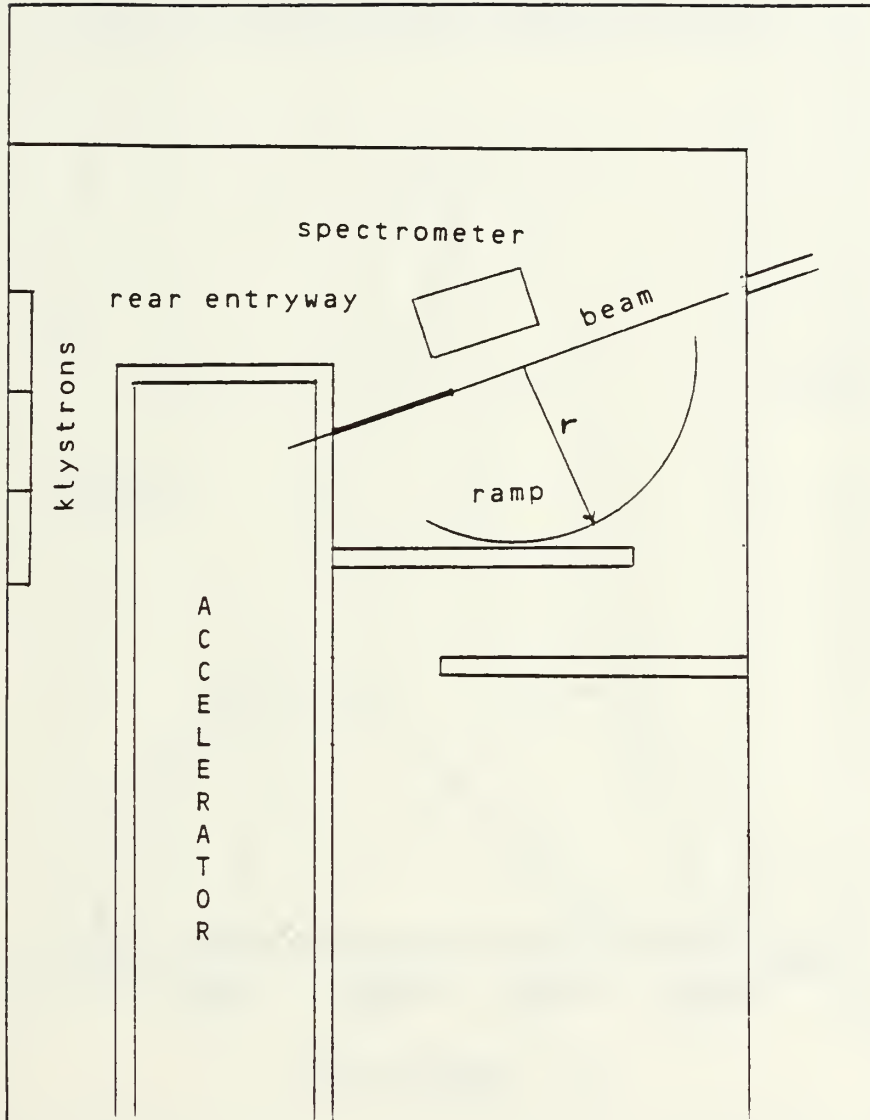


Figure 2 The NPSAL Experiment Station

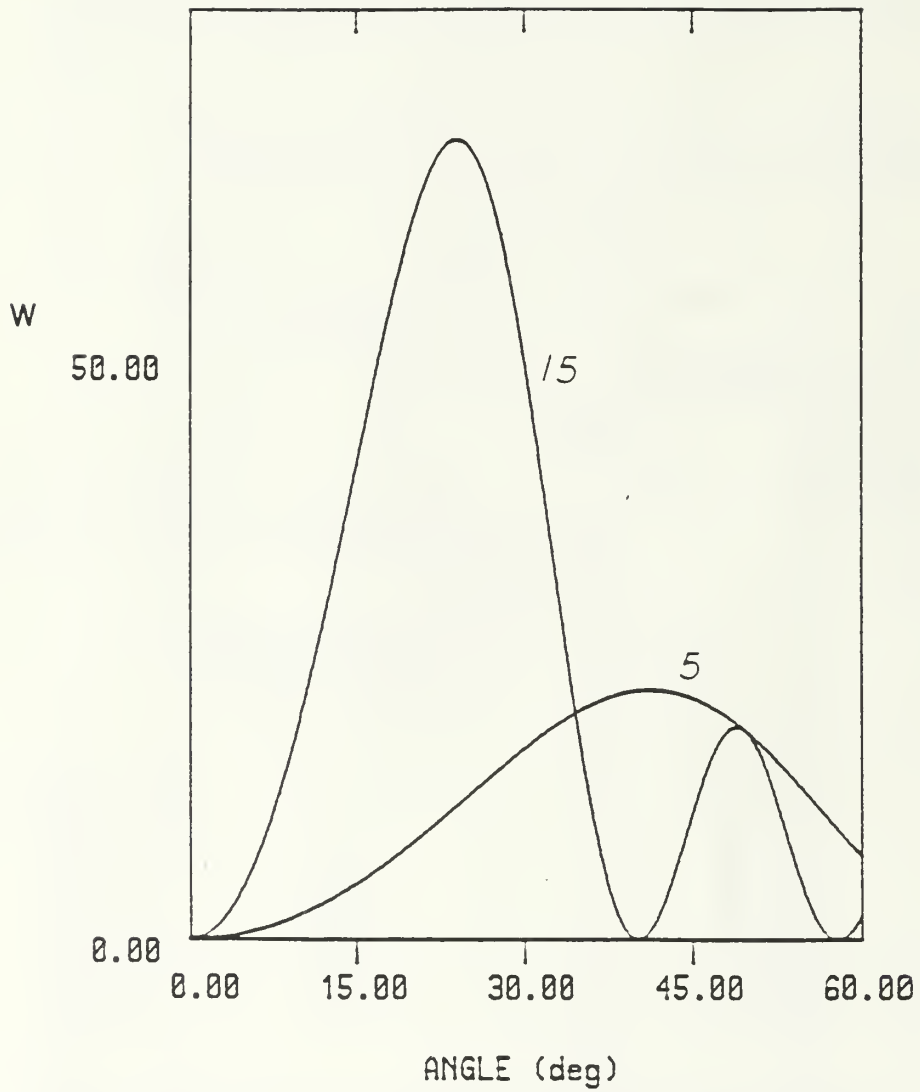


Figure 3 Third Harmonic curves where $L=15$ cm
and $L=5$ cm

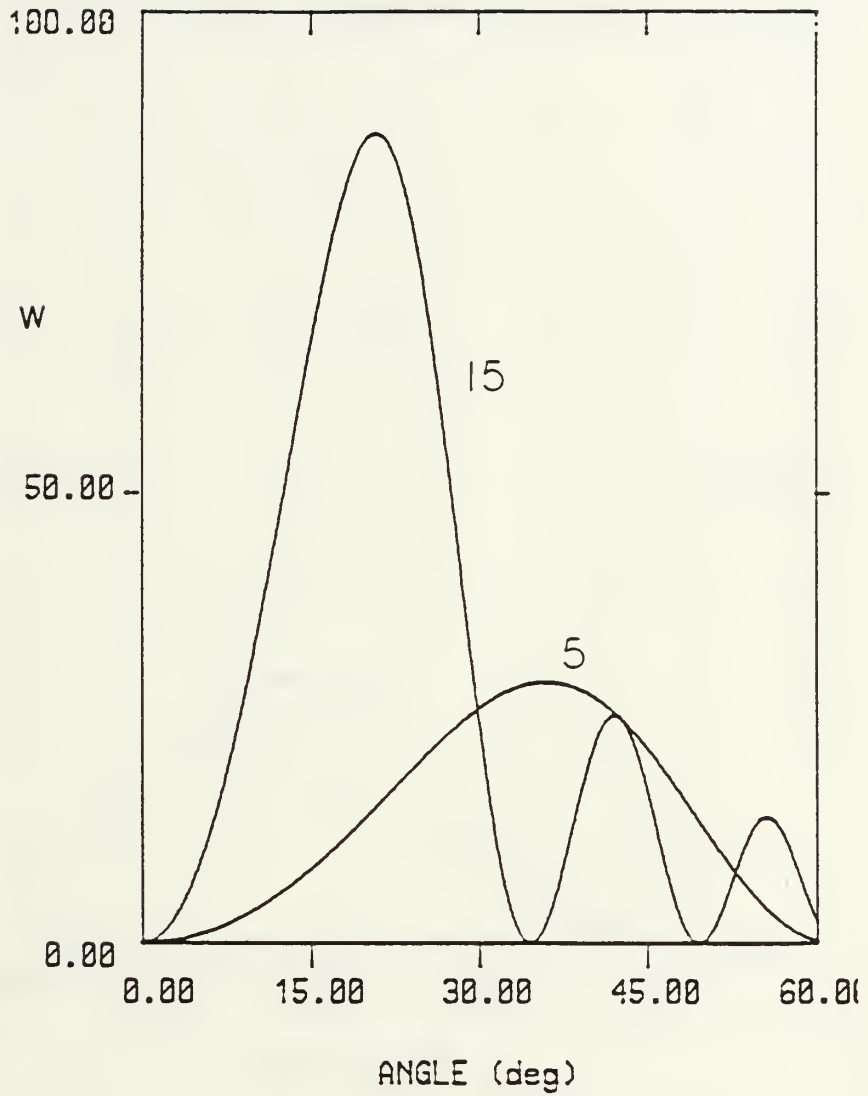


Figure 4 Fourth Harmonic curves where $L=15$ cm and $L=5$ cm

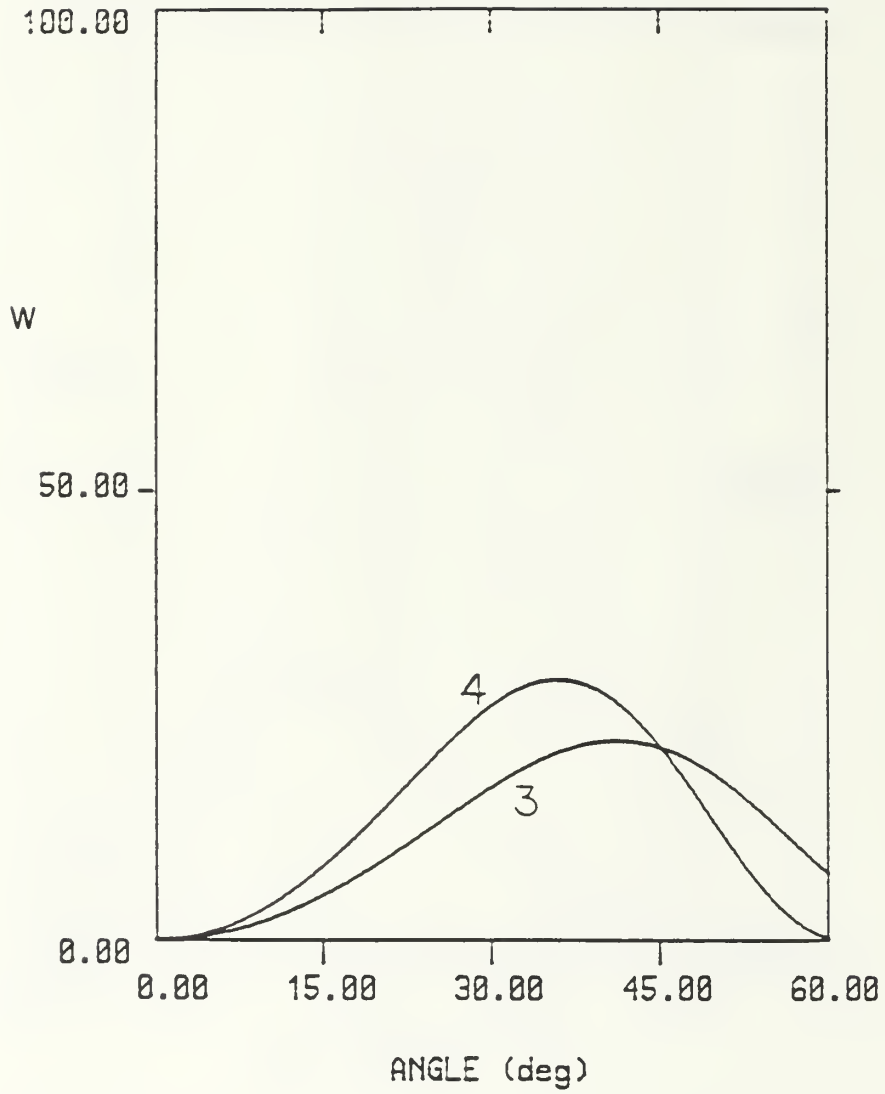


Figure 5 Third and Fourth Harmonics
where $L=5$ cm

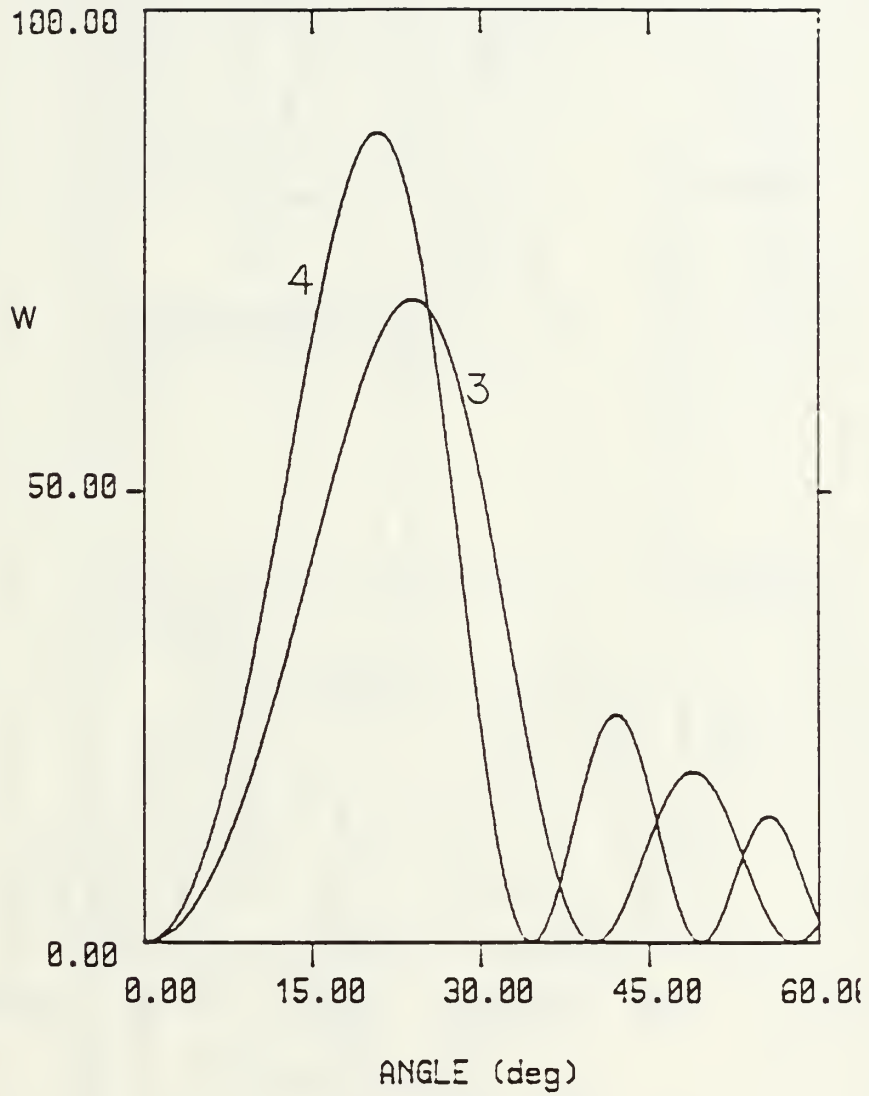


Figure 6 Third and Fourth Harmonics
where $L=15$ cm

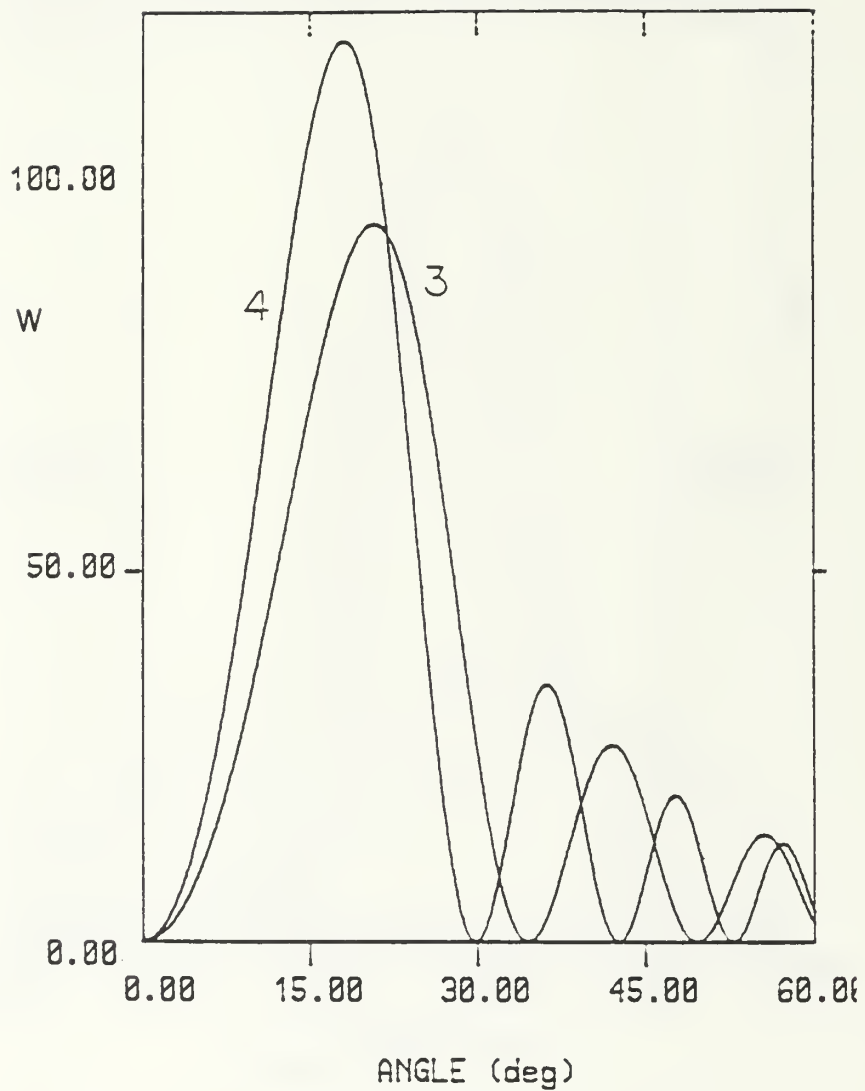


Figure 7 Third and Fourth Harmonics
where $L=20$

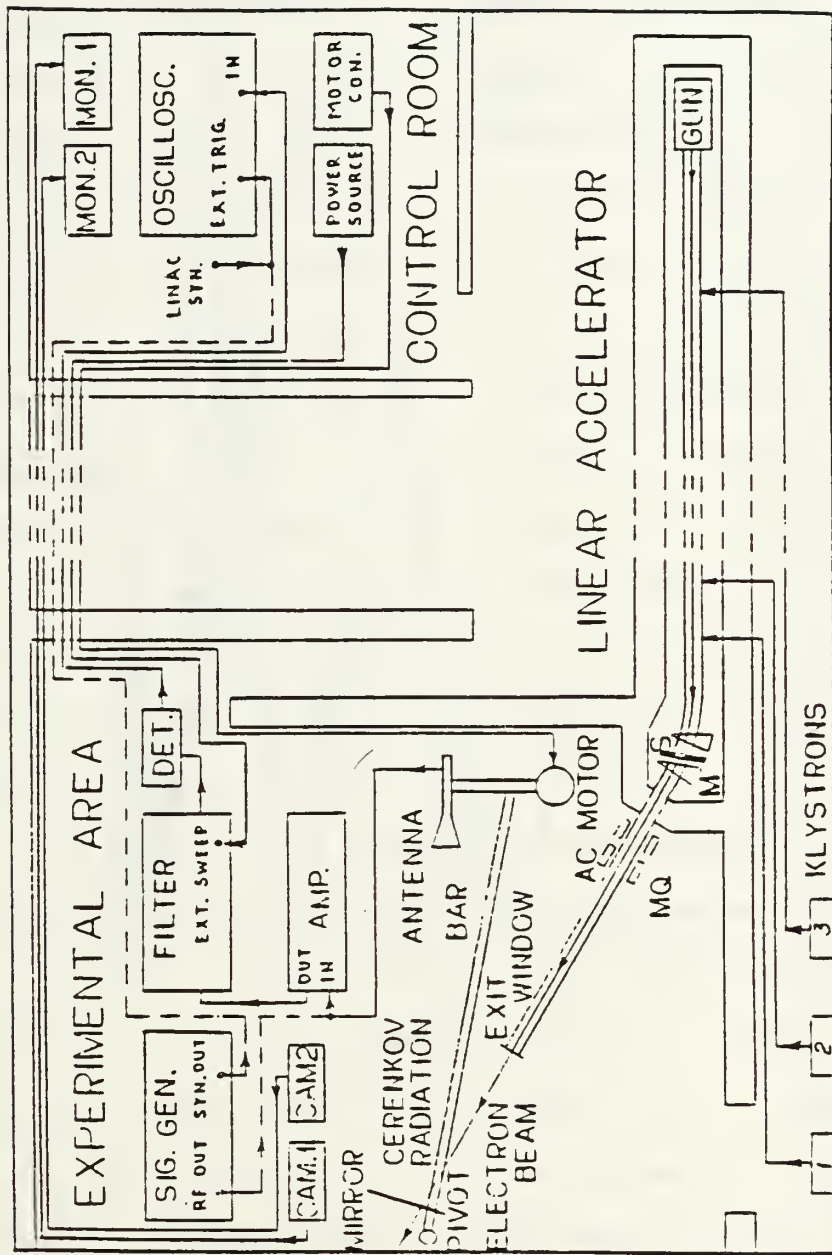


Figure 8 Vujaklija's Experimental Setup

NPSAL? Indeed this has been the topic of several recent experiments at NPSAL.

B. PREVIOUS EXPERIMENTS

In 1982 Saglam [Ref. 7] did an experiment to look at X band and K band Cerenkov radiation for interaction lengths ranging from 66 to 89 cm. His results were the first experimental confirmation that Cerenkov radiation occurs at angles larger than that expected from calculating the Cerenkov angle of 1.3 degrees [Ref. 8].

In 1983 Newton [Ref. 9] looked at several harmonics and combinations of harmonics from the 3rd to the 7th using an interaction path length of one meter. Since Newton's path length, like Saglam's, was proportional to the distance of his field point, his measurements were not in the far field and, therefore, the results would have been ambiguous for angles of theta greater than a few degrees. Newton thus limits his measurements in each case to the first lobe. His results follow Saglam's in showing initial confirmation of the theory.

In 1984 Vujaklija [Ref. 5] did a similar set of experiments but reduced the finite length to 0.14 meters in order to take measurements in the far field. To compensate for the loss of power due to the reduced L, Vujaklija used a traveling wave tube amplifier (TWT). He also used a tunable YIG filter to isolate the desired harmonic (Figure 8).

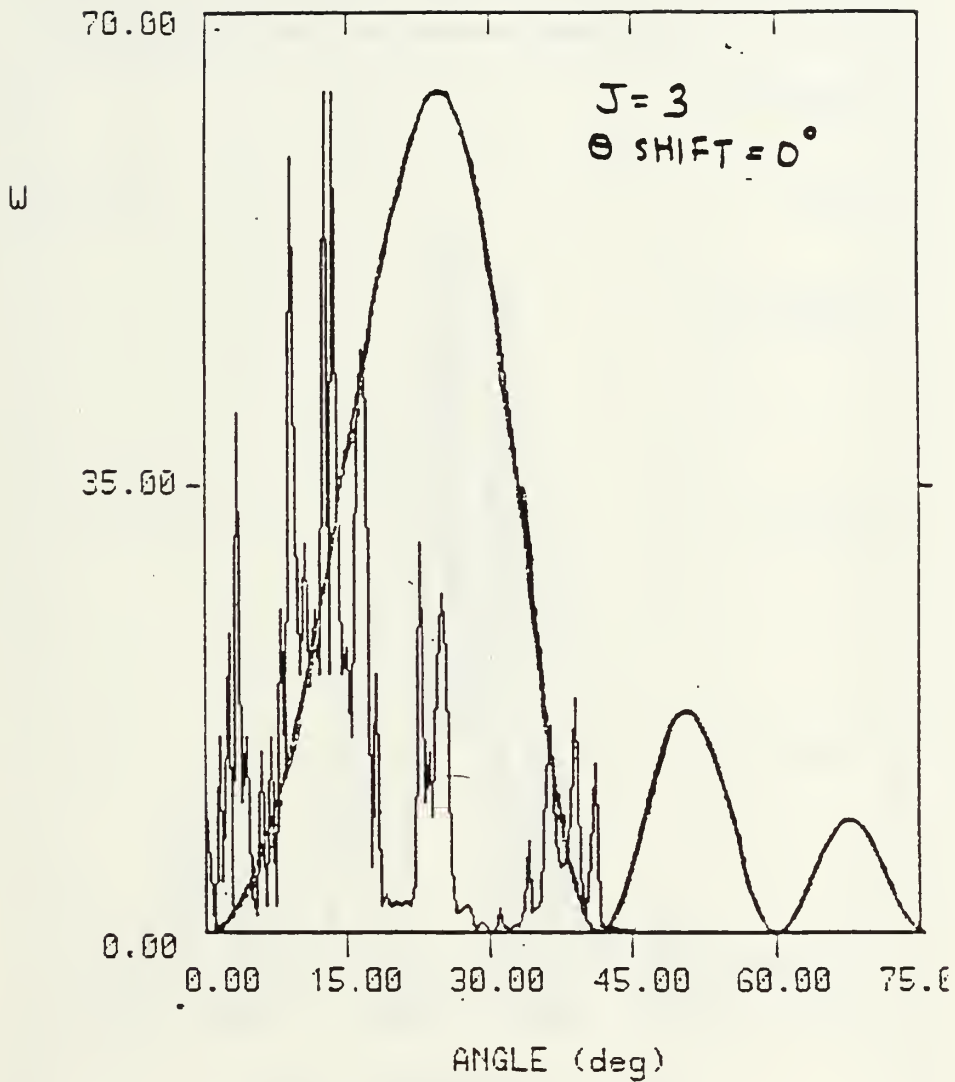


Figure 9 Vujaklija's Data using the Mirror for the Third Harmonic with no Shift in Angle

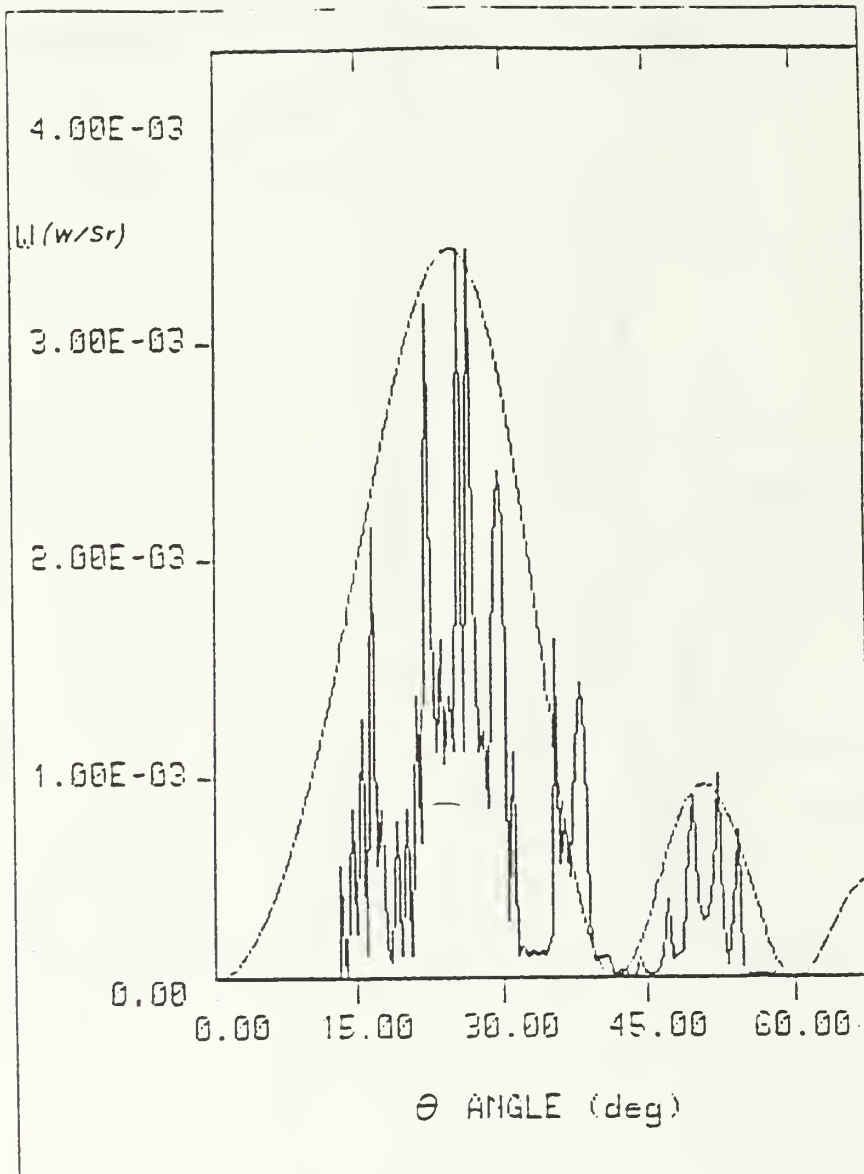


Figure 10 Vujaklija's Data using the Mirror for the Third Harmonic with an angular shift of 13 degrees

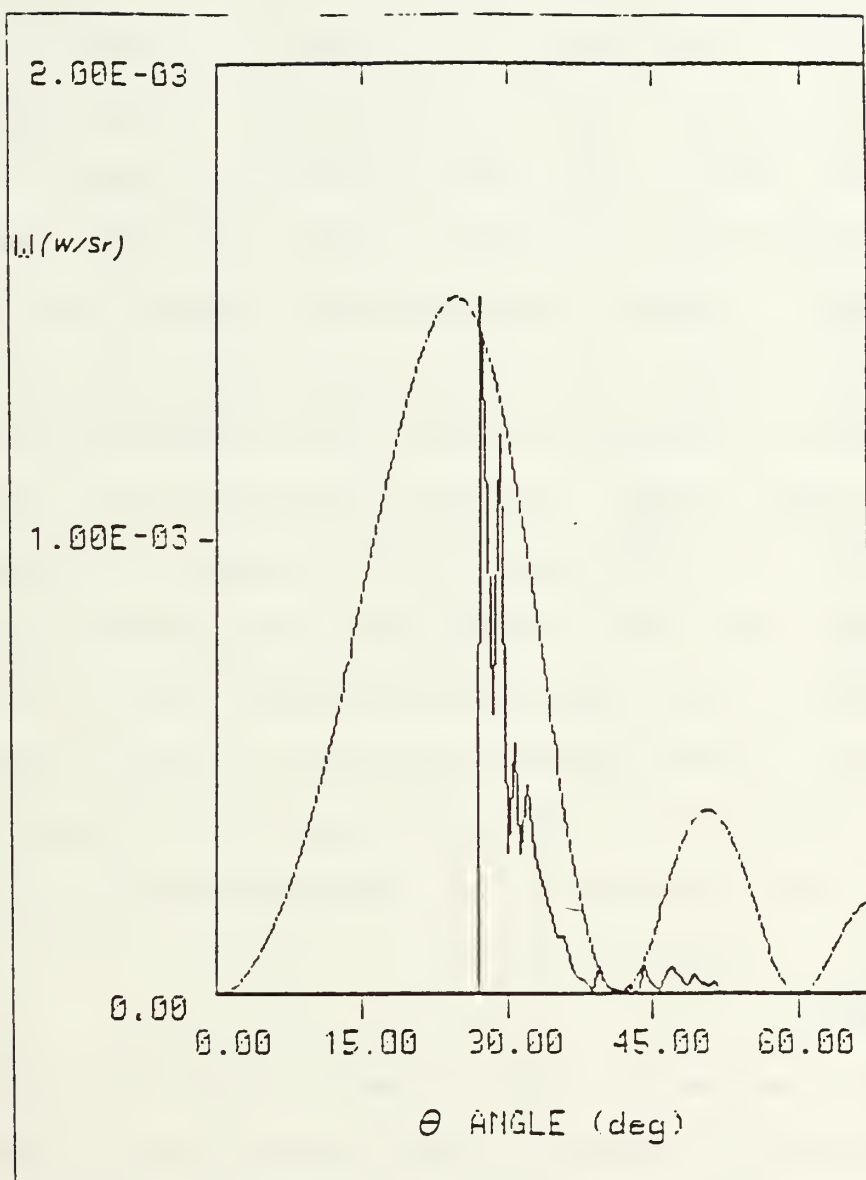


Figure 11 Vujaklija's Data without the Mirror for the Third Harmonic

Vujaklija's findings report unexpected spikes or fine structure in the radiation pattern. Figures 9 and 10 show his results for an experiment in the third harmonic compared to the theoretical curves. The data for these figures was taken while using a mirror in the beam path. In Figure 9 there is no angular shift in the data, while in Figure 10 the data is shifted thirteen degrees. Note that the spike envelope approximately follows the smooth theoretical curve. Vujaklija speculated that the spikes were caused by noise interference and concluded that with an effort toward noise reduction they could be eliminated. Figure 11 shows the result of yet another experiment by Vujaklija, but this time the data was gathered from direct measurements with improved shielding. Note the slight reduction of noise between this data in Figure 11 and that shown in Figures 9 and 10. This experiment showed that the angular shift of the earlier measurement was an artifact induced by the use of a mirror.

C. PURPOSE

This experiment, while aimed at confirming Equation 1, is primarily focused on reducing noise so that data can be taken reliably and the fine structure due to interference can be eliminated. A secondary focus is to improve the method of recording data. The data presented in this thesis shows that the spikes which appeared in Vujaklija's

experiment are essentially absent after the experiment is shielded from unwanted noise.

II. THE EXPERIMENT

A. EXPERIMENTAL SETUP

The experimental setup shown in Figure 12 is generally similar to the setup used by Vujaklija reported in Reference 5 and illustrated in Figure 8. In the experiment station a microwave horn antenna with a short section of wave guide is set in the far field of, and aimed at, the interaction beam length (L). The antenna is mounted to a dolly which travels in an arc at radius (r) around the interaction beam length at an angle relative to the beam path. The Cerenkov radiation, after being reflected off a mirror in the beam path, is seen by the antenna as a function of the angle to the beam. Figure 13 illustrates the mirror geometry. The Cerenkov signal then travels through a short piece of coaxial cabling to a traveling wave tube amplifier (TWT) and then to a crystal detector for demodulation before it travels the twenty-five meters through a triply shielded cable to the control room. Figures 14, 15, and 16 display the propagation characteristics of the various components from the waveguide to the TWT. Once at the control room the signal is split and sent in two directions. One direction leads to an oscilloscope for viewing, and the other to the recording network which includes an amplifier,

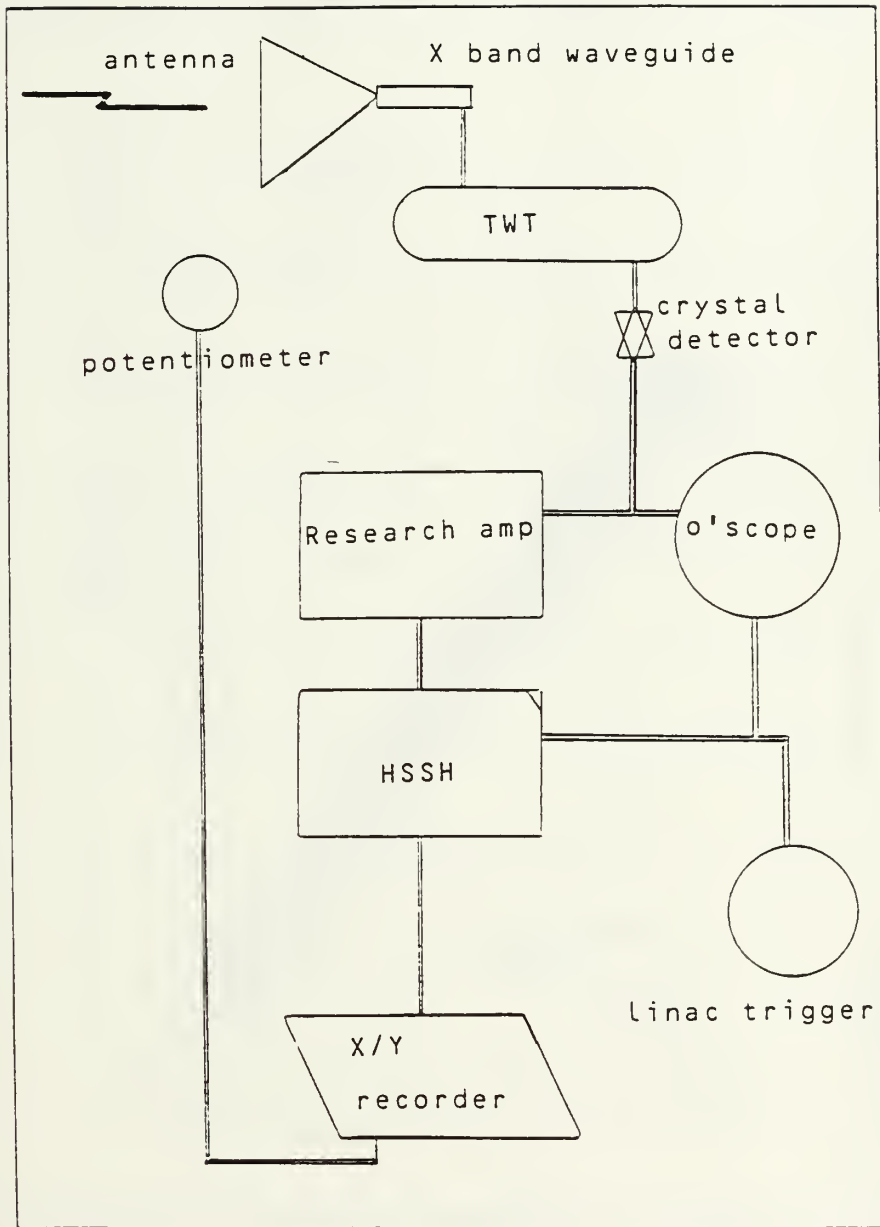


Figure 12 Experimental Setup

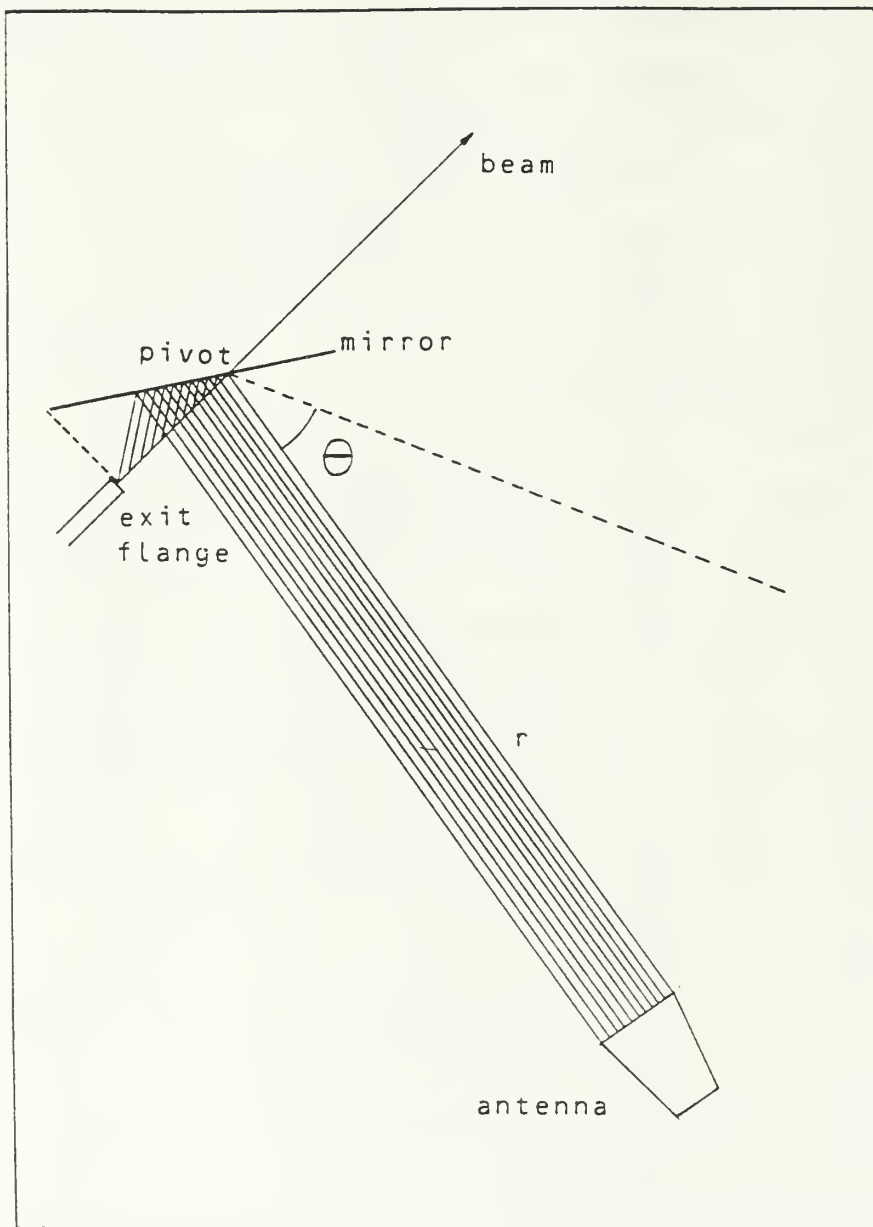


Figure 13 Mirror Geometry



Figure 14 Attenuation Data on X Band Waveguide

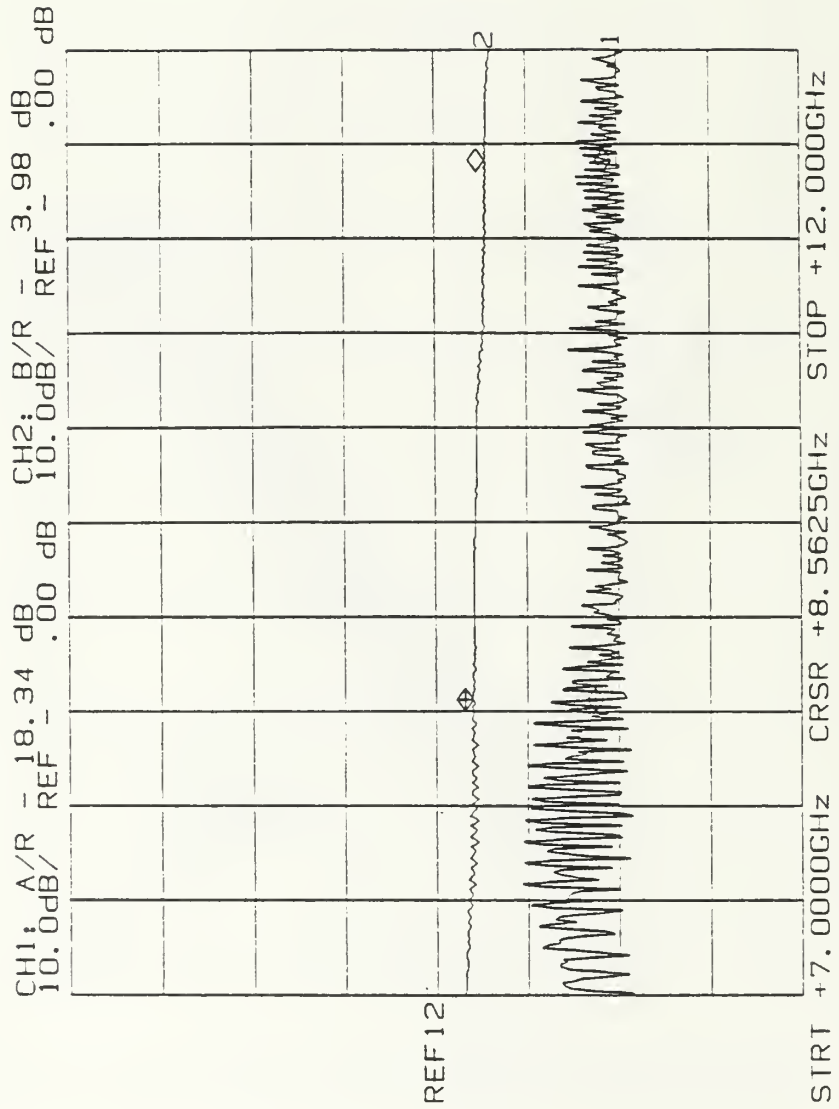


Figure 15 Attenuation Data on RG 9/U Coaxial Cable

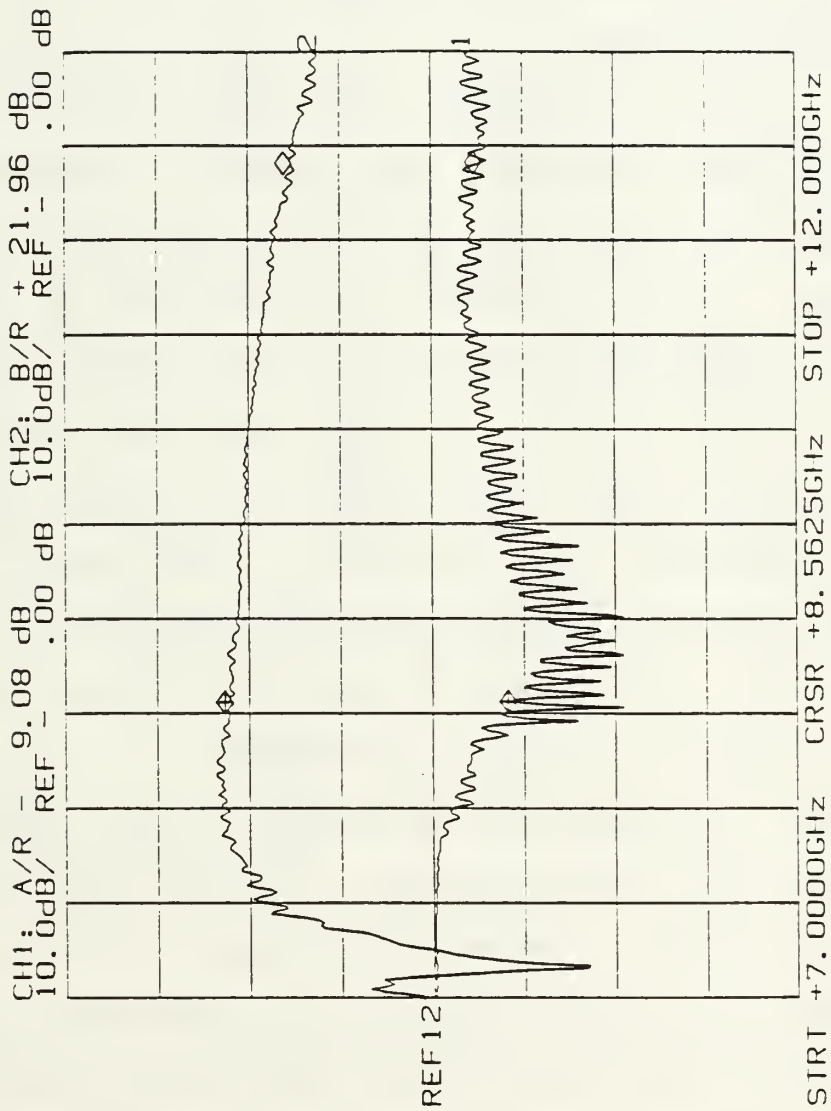


Figure 16 Attenuation Data on the System from the Waveguide through the TWT

an IC high speed sample and hold network (Figure 17), and the X/Y recorder. Figure 18 illustrates the morphology of the signal from the beam to the X/Y recorder. Appendix A contains a more detailed description of each piece of equipment used in this experiment.

B. NOISE REDUCTION

The linear accelerator generates a fair amount of residual radio frequency (RF) noise. Therefore, the experiment room at NPSAL is not the ideal place to do an experiment which involves the detection of low power Cerenkov microwave radiation from a small interaction beam length. The walls, the floor, and the ceiling, all intrinsically good reflecting surfaces by themselves, contain fixtures which make for a complicated array of reflecting surfaces. The spectrometer magnet alone, standing within fifty centimeters of the beam, offers two square meters of metallic reflecting surface.

Noise is defined here as undesired radio frequency (RF) emissions which interfere with, and in some cases drown out, the desired signal. Noise, for purposes of this experiment, can generally be classified into two categories. The first is noise received directly at the detecting antenna, and the second is noise that is picked up by the triply shielded cabling which joins experiment room apparatus with control room apparatus. The first category, noise picked up by the

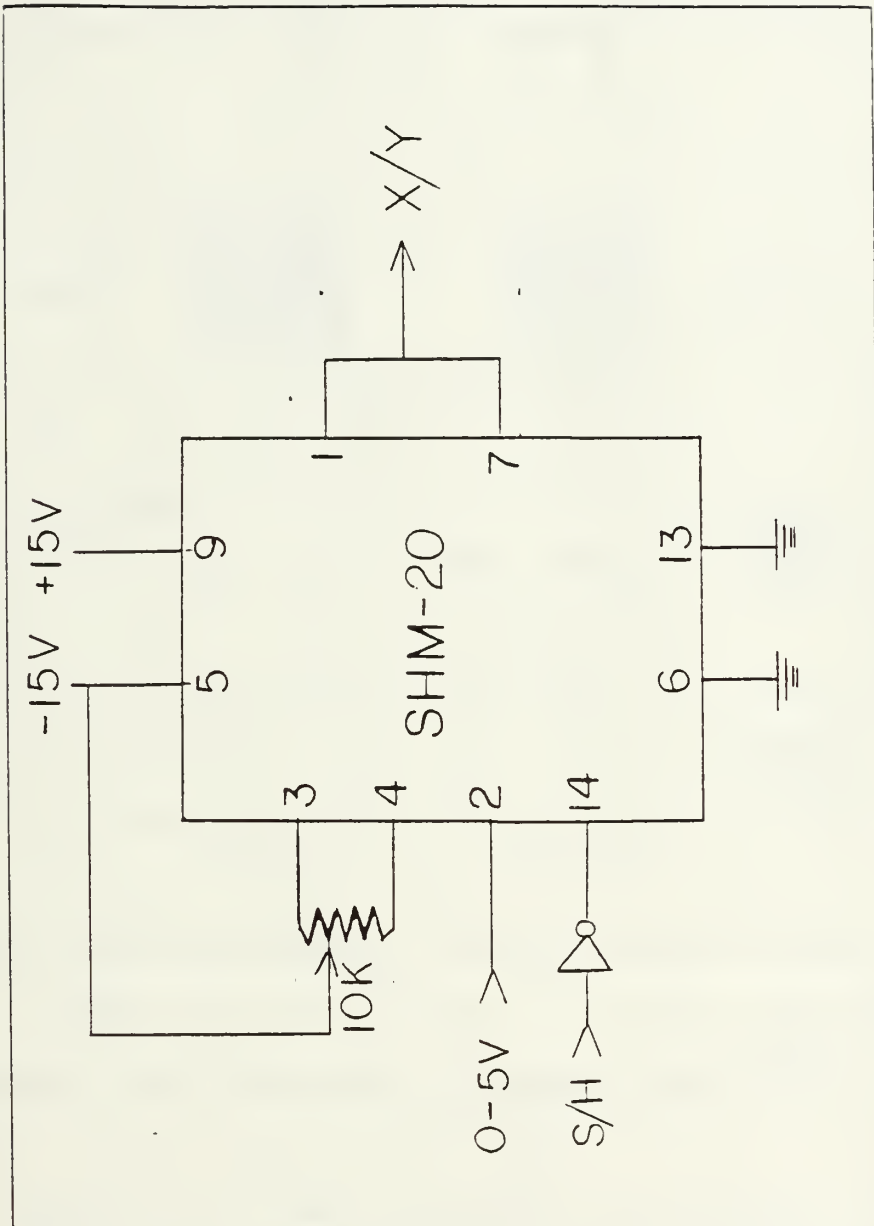


Figure 17 High Speed Sample and Hold Network

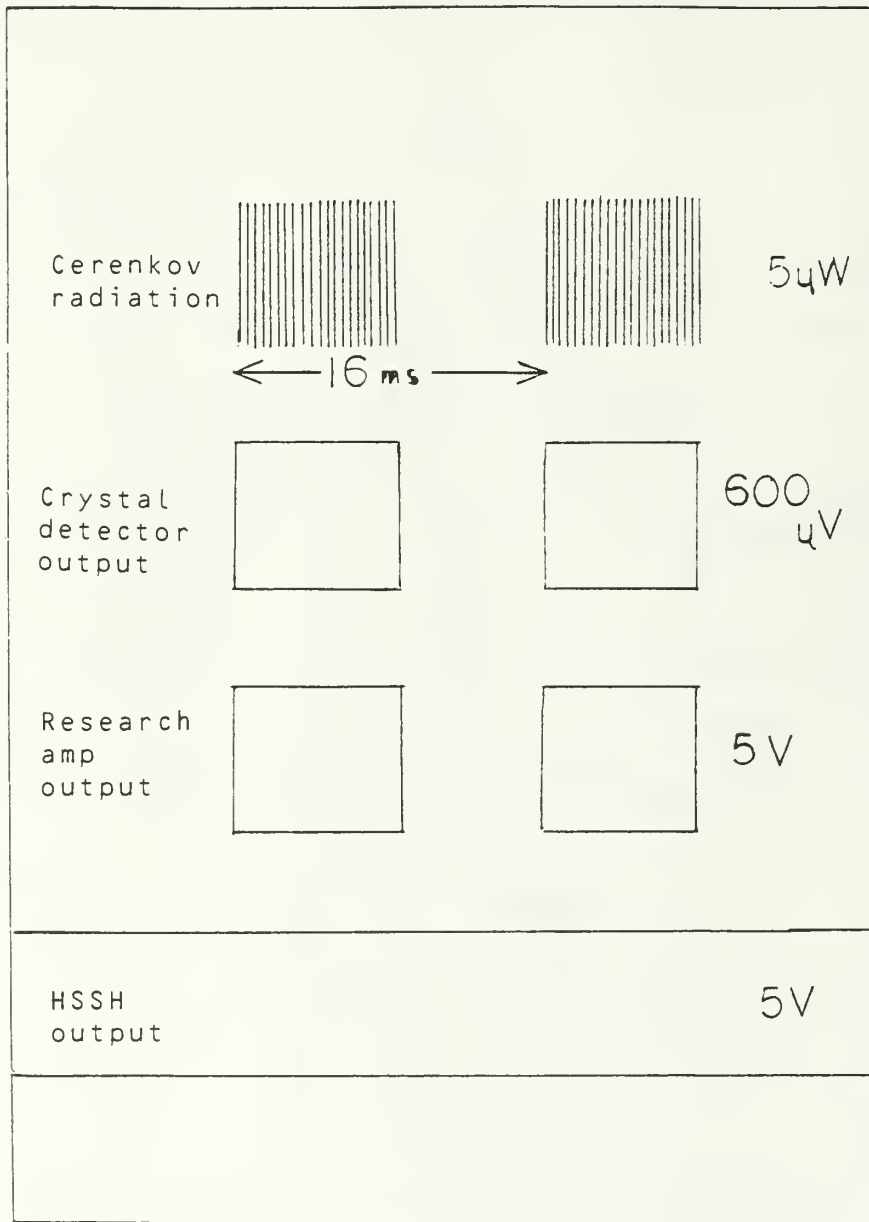


Figure 18 Signal Morphology from Beam to X/Y Recorder

antenna, can be further divided into two subcategories: 1) Cerenkov radiation received by the detector after it has been reflected off secondary objects in the experiment station, and 2) klystron noise received at the detector which propagates through the rear entryway of the experiment room. A diagram of the experiment room is shown in Figure (2).

The reflected Cerenkov signal, the first subcategory of noise, even when falling off as $1/r^2$, can still reach the detector with power appreciable enough to mask any nulls or suppress any peaks in the signal coming directly from the interaction length. Figure 19 shows a map of the signal at the detector during a sweep from about ninety degrees angle to the beam to about about one hundred thirty degrees. During this sweep a one foot by four foot sheet of aluminum plate was present against the wall on the opposite side of the beam from the detector. Figure 19 also shows a sweep after the plate had been removed. A comparison between the two sweeps shows that the reflected signal has a large influence on the shape of the radiation pattern. A beam cover (Appendix A) was also used in the noise reduction phase of the experiment with the idea of eliminating down-beam Cerenkov radiation.

The second subcategory of noise which is received at the detector emanates from the klystron bank. Figure 20

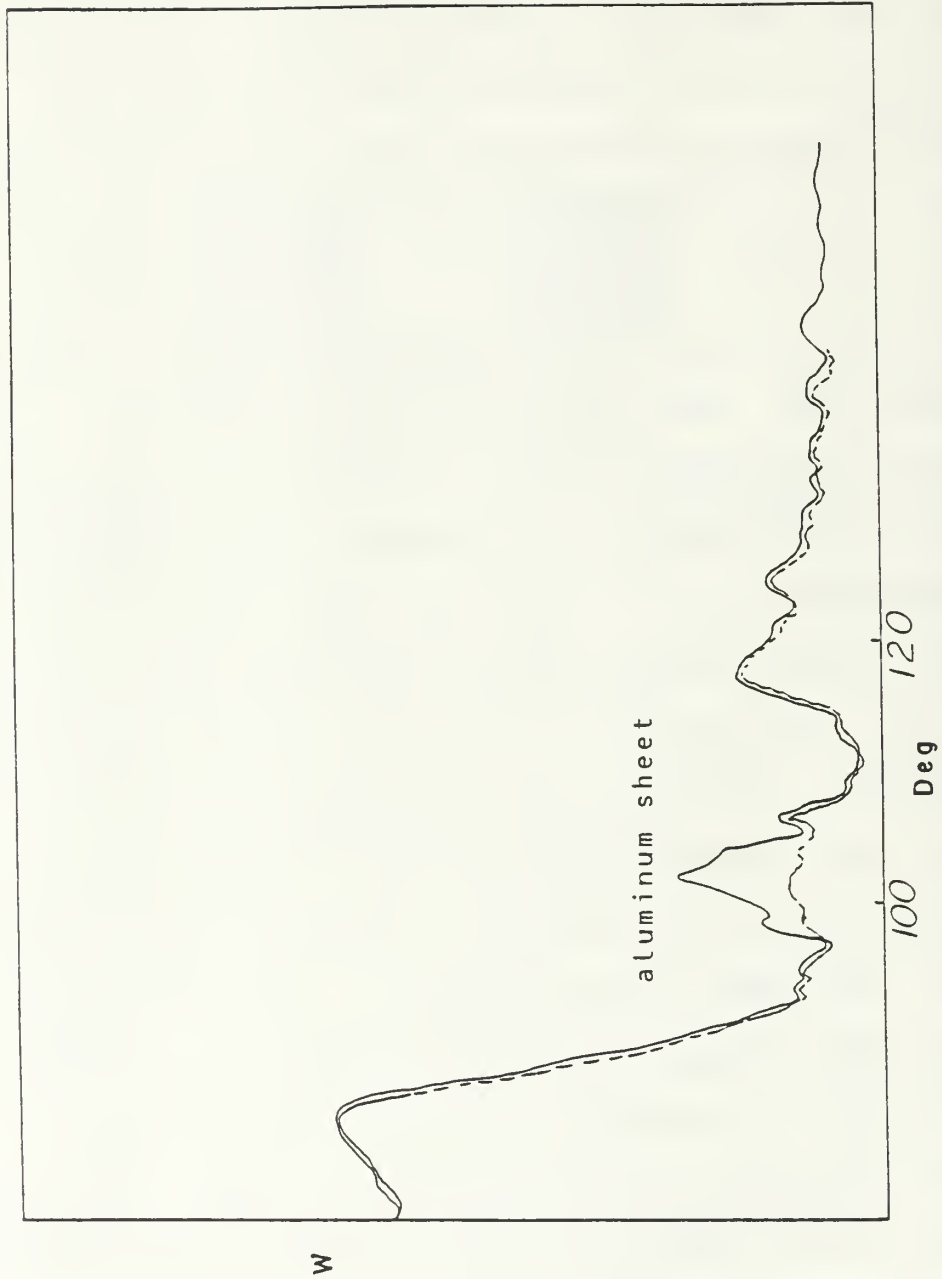


Figure 19 Reflected Noise

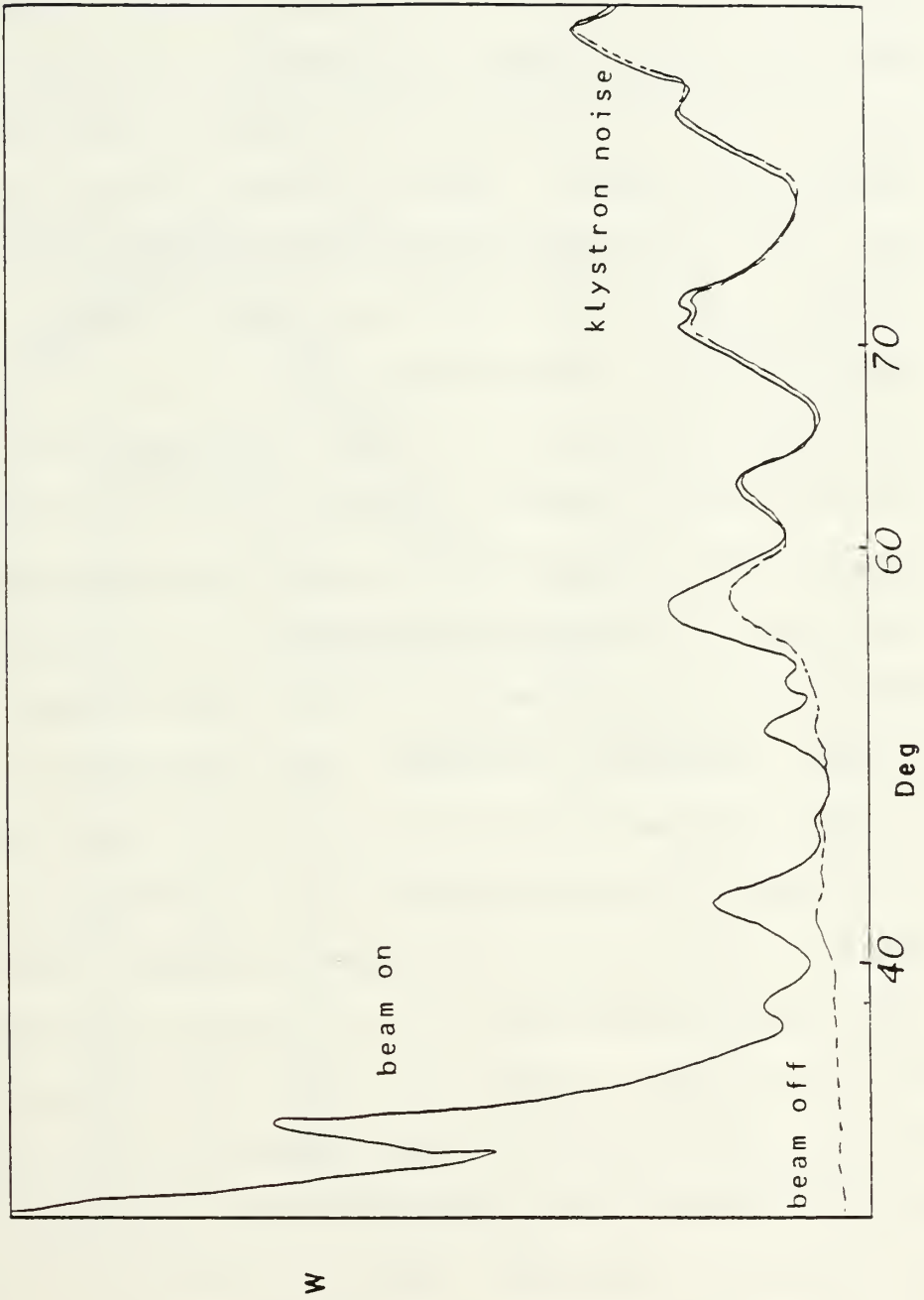


Figure 20 Klystron Noise

shows two patterns, one taken when the beam was on and the other when the beam was off. The beam on pattern shows a beam induced radiation while the other pattern, taken while the beam was off, shows an absence of beam induced radiation. The klystron noise is present in both patterns and remains unchanged. Both patterns show that the magnitude of the klystron noise depends on the position of the antenna. Klystron noise is greater at higher angles with reference to the beam path because it is in that position that the detector is "looking" in the direction of the the klystron bank beyond the rear entryway. The power of the klystron noise in the third harmonic was measured at the position shown in Figure 21 and read one microwatt. This represents ten to twenty percent of the peak Cerenkov signal for the same frequency. A copper mesh was placed over the entire rear entryway cutting the noise to a level where it could no longer be detected above the -45 dBm noise floor. Additionally, some airmat microwave absorber (described below) was placed around the walls of the rear entryway.

The other major category of noise, RF energy being picked up by the cabling, is the reason for not using the tunable YIG filter to isolate the desired harmonic while mapping Cerenkov radiation. The YIG filter has a -8 dB insertion loss that brings the desired signal down to levels which do not allow the high speed sample and hold circuit to

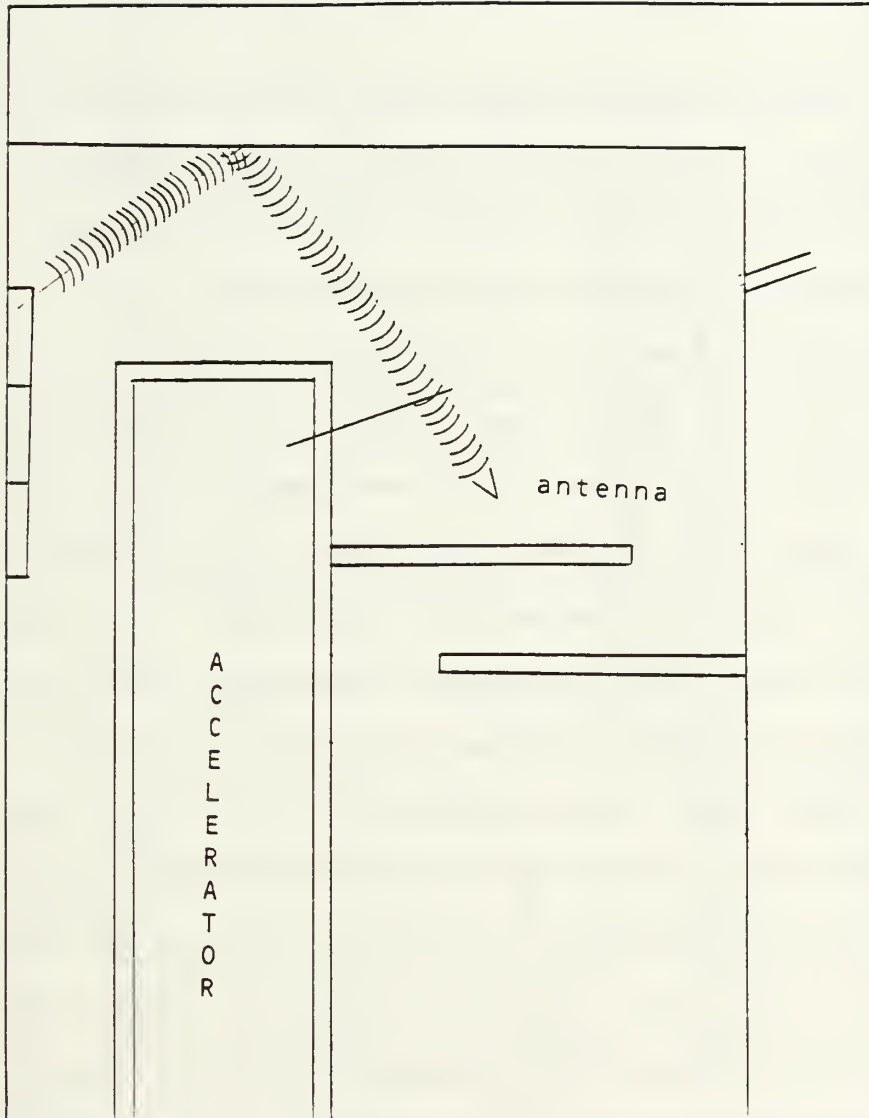


Figure 21 Antenna Position for Measuring Klystron Noise

distinguish it from the cable noise. Therefore, unlike Vujklija's thesis, the YIG filter cannot be used to collect Cerenkov radiation data. It can, however, be used to check for the presence of other harmonics as will be explained below.

The success of this experiment in verifying Equation 1 is dependent on a) reducing the radiation noise at the detector to levels below that of the direct Cerenkov signal, and b) minimizing the noise in the cabling.

To reduce noise in the experiment station all portable metallic objects which came into view of the antenna were removed from the room. The non portable metal which provided good reflecting qualities were covered with a microwave absorbing material available in sufficient quantities from the Microwave Laboratory at the Naval Postgraduate School. Another absorbing material of blue sponge rubber was also available but not in sufficient quantities. Figure 22 shows the absorbing characteristics of both types of materials. The highest curve in Figure 22 represents the power of the reference signal (0.0 dBm) reaching the receiver via transmit and receive antennas placed ten inches apart. The center curve represents the same setup with the addition of a sheet of airmat placed in the ten inch gap. Note that the signal attenuation is close to 17 dB. The lowest curve located at the noise floor is

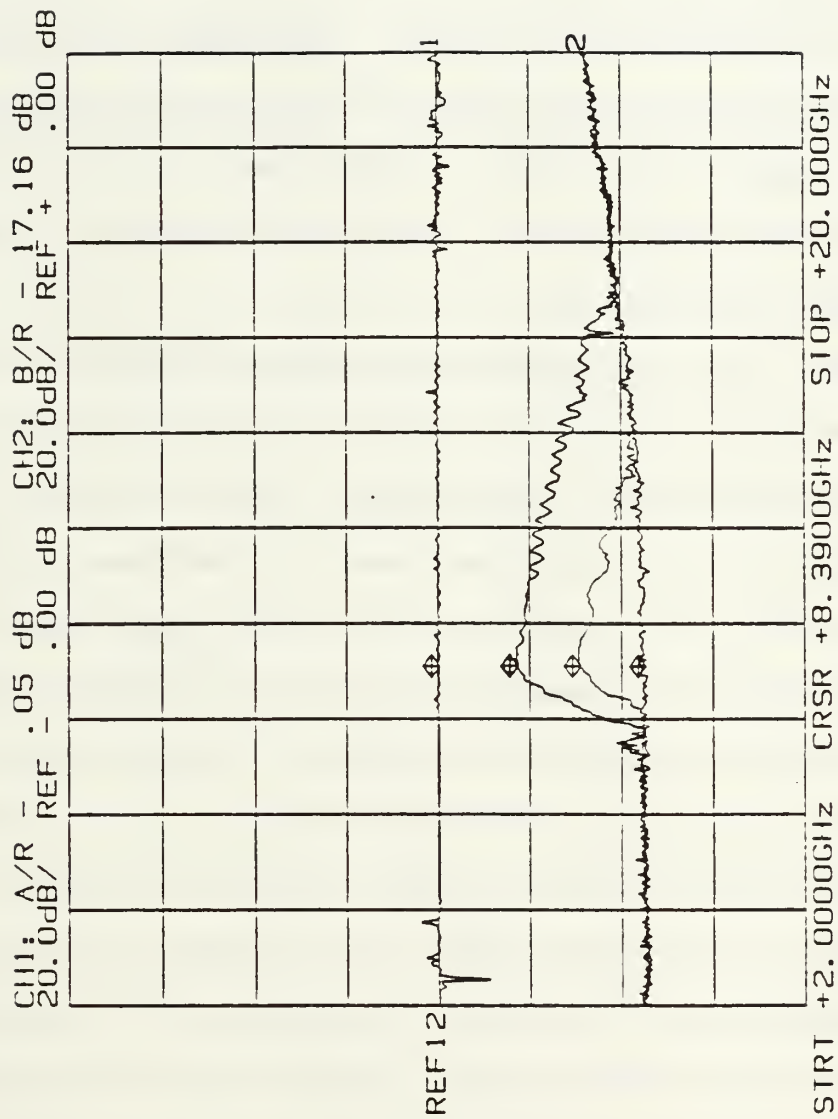


Figure 22 Absorbing Characteristics of Two Types of Microwave Absorbers

the signal with the blue sponge absorber in the ten inch gap. Airmat shielding was placed around the rear entryway, around the spectrometer magnet, around the beam dump, along the walls, and around the exit window.

The extensive shielding resulted in reducing not only the reflected Cerenkov signal, but also the klystron noise. The problem of the RF noise in the triply shielded cabling was partially corrected by grounding the cabinetry of the electronic equipment used in the experiment.

C. COLLECTING DATA

Early in the experiment data was taken using a 30 MeV beam which proved useful only toward solving the problem of noise reduction. Otherwise, for recording Cerenkov radiation the thirty MeV beam was unproductive. It was during this early phase that the sample and hold circuit was installed for the improved method of recording data. In all experiments mentioned earlier in this paper data was gathered by manually recording values from the oscilloscope or from the spectrum analyzer at angles observed through the closed circuit television. This method of collecting data was subject to uncertainties resulting from instabilities in the linac over the lengthy time period it took for a sweep of a given angle of theta. The speed of the sweep, not counting the time to stop and record data, was about 5 degrees per minute. With the X/Y recorder method a single

sweep of seventy-five degrees in theta takes less than twenty seconds, and the data was recorded automatically by the X/Y recorder. Over this time period the data inconsistencies caused by the linac instabilities are reduced significantly compared to the manual method.

A series of experiments were run to reduce noise until the point was reached when Cerenkov radiation data could be duplicated in successive runs. This was a significant breakthrough in the experiment - the focus shifted to Cerenkov radiation and away from the ancillary problems.

All of the significant runs to map Cerenkov radiation were done with the mirror, without a beam cover, and with a 100 MeV beam. Collecting data without the mirror was discontinued because of two problems which were common to previous experiments as well as this one: 1) The antenna could not be moved directly into the beam and therefore the first lobe in the diffraction curve could not be recorded, and 2) L could not be defined with reliability. Masking the area defined as L interrupted the signal path for low angles of theta. The mirror provided a reliable solution to these problems. The geometry in Figure 13 shows that the antenna sees a well defined L from a wide range of theta. As long as the projection of the mirror onto L is equal to or greater than L, L does not change with theta until high angles where the reflection of L is masked by the exit

window flange. If the projection of the mirror is less than L , then at some angle in theta L will begin decreasing as theta increases.

The beam cover was not used in the final experiments because shielding elsewhere in the experiment room served as well.

The harmonic for the final experiment was $j = 3$ as indicated by the 6.2 dB loss between the two harmonics as illustrated in Figure 16. Additionally, during the experiment, the YIG filter was inserted in the system to determine which harmonics were being propagated. The YIG did not show any $j = 4$ signal, but did show a prominent $j = 3$ signal. Figure 23 illustrates the relative signals reduced from photographs.

The Cerenkov radiation data collected from the final experiments are shown in Figures 24 through 27. For Figures 24 through 26 L was measured as the distance from the exit window to where the beam strikes the mirror at 14.0 cm. and for Figure 27 L was measured at 16.5 cm. The angular scale at the bottom of the graphs show a real angle to the beam and a data angle to the beam. The real angle represents the position of the antenna despite the mirror and the data angle represents the angle to the beam reflected off the mirror. The zeros of the data angle (reflected beam path)

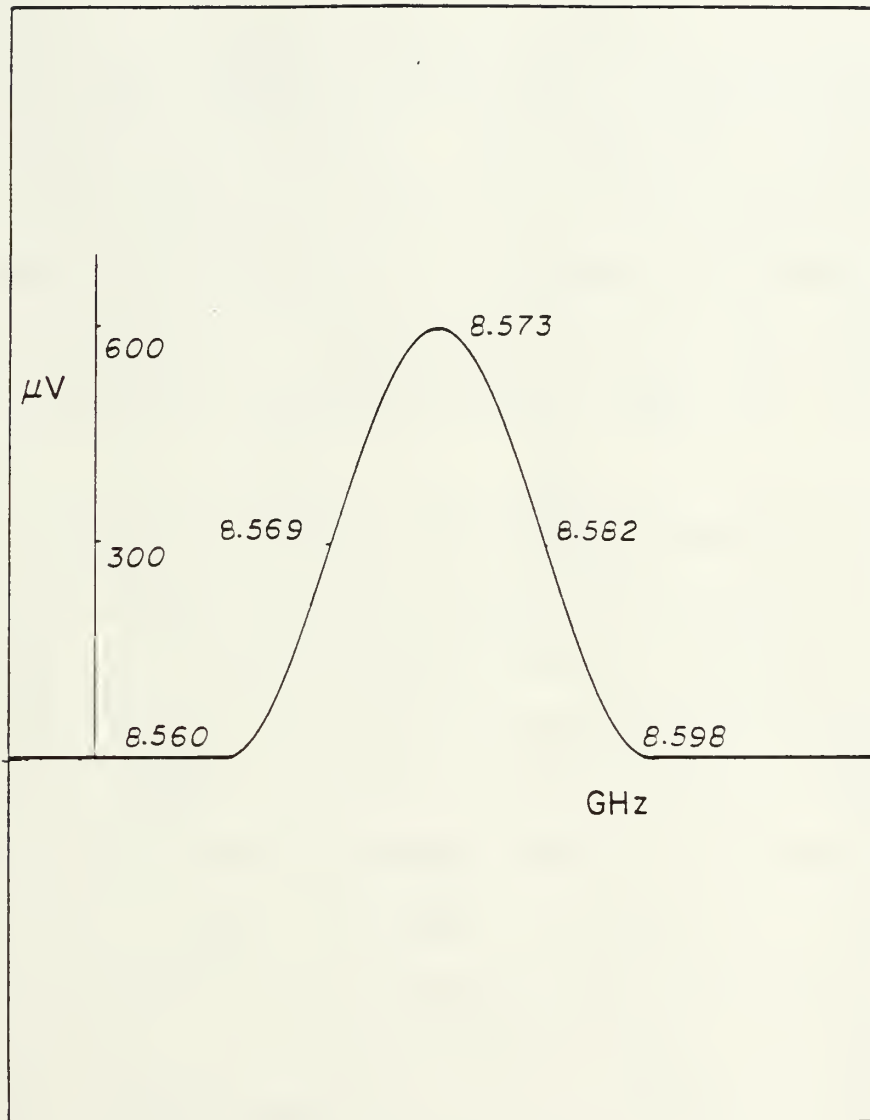


Figure 23 YIG Data for the Third Harmonic

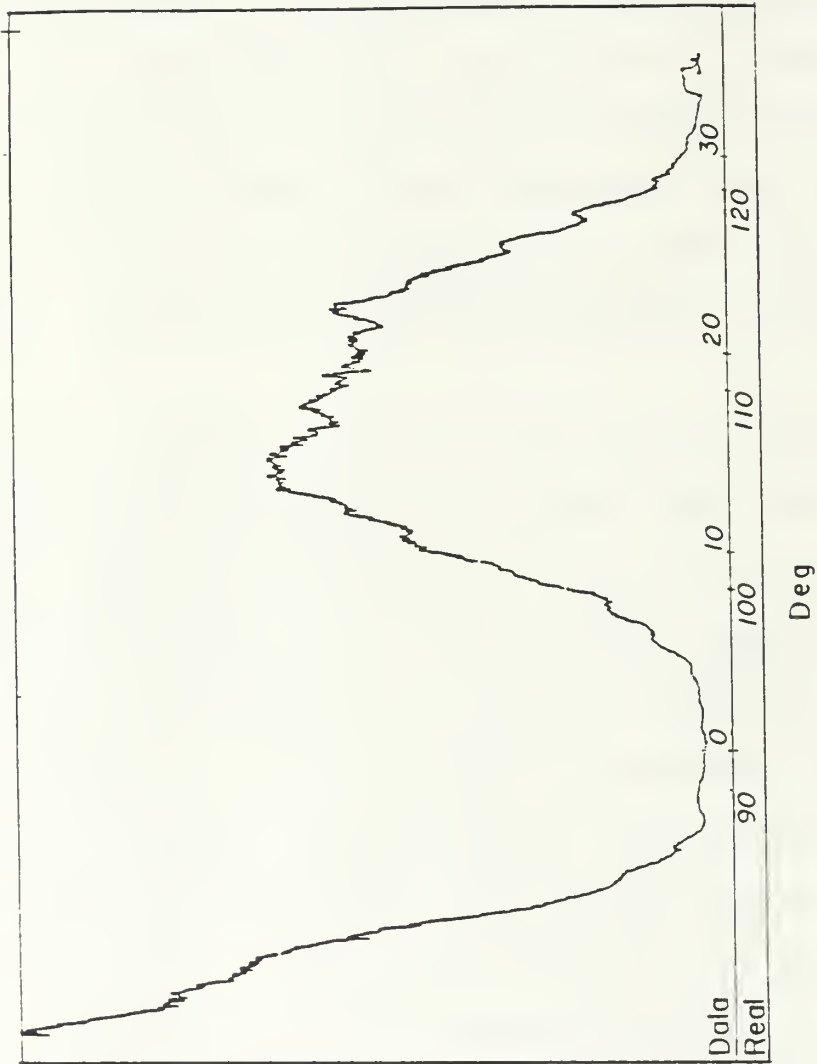
are taken at the centers of the nulls between the left and right hand lobes.

III. RESULTS AND CONCLUSIONS

A. RESULTS

The Cerenkov radiation data shown in Figures 24 through 27 are similar in structure. They show two major lobes (one from each side of the beam) and an area between the two lobes wherein the zero angle to the beam is located. Only the right hand lobe, representing radiation from the left side of the mirror looking down-beam (Figure 13), will be discussed.

There are also several variations between the data. Note that the major lobes in Figures 24 through 26 shift successively to the left in real angle to the beam. This is because the angle of the mirror to the beam was adjusted to the left, or counter clockwise, with each run. Note also that none of the lobes are symmetrical. In Figures 25 and 26 there is an aberrant slowing of the positive slope about midway to the peak, and in Figure 25 the slope actually goes negative briefly. In Figure 24 the aberration is apparently absent but is likely enveloped in the major lobe. The cause for this asymmetry is not understood, but the most likely reason is mirror generated noise not constant in angle to the beam.



W

Figure 24 Cerenkov Radiation for the Third Harmonic and Where L is Measured at 14.0 cm

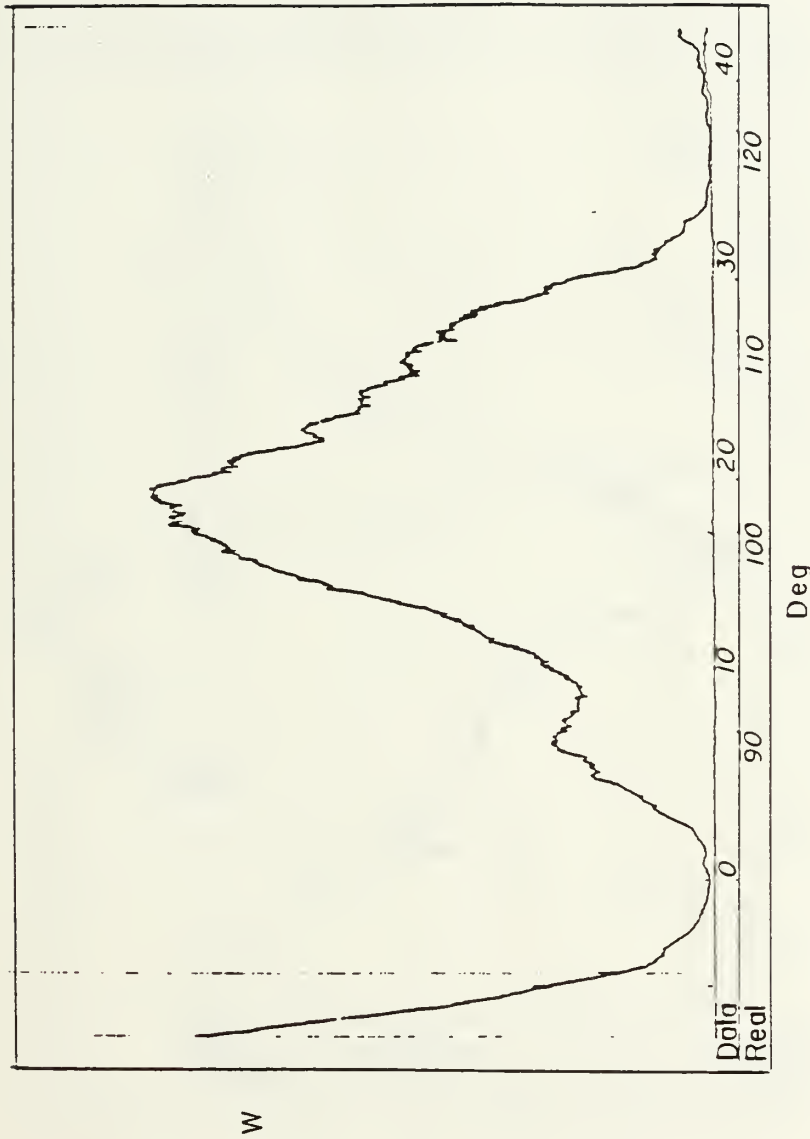


Figure 25 Cerenkov Radiation for the Third Harmonic and Where L is Measured at 14.0 cm

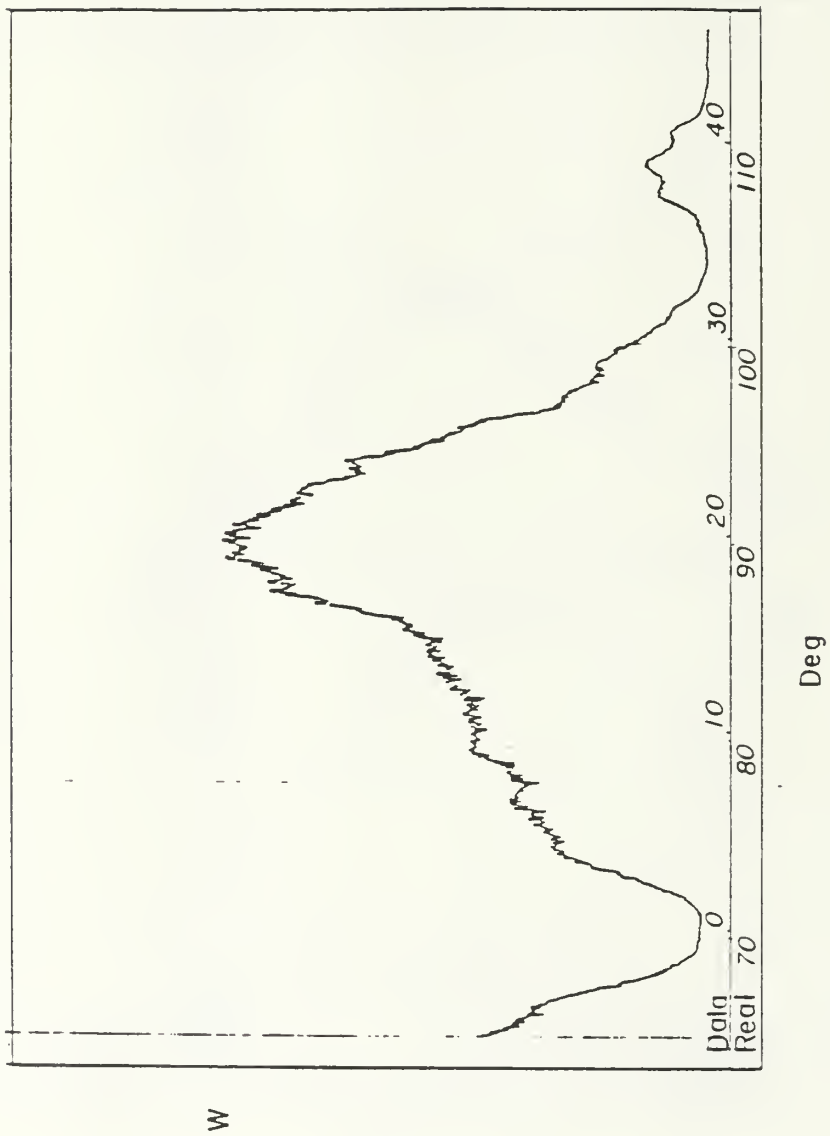


Figure 26 Cerenkov Radiation for the Third Harmonic and where L is Measured at 14.0 cm

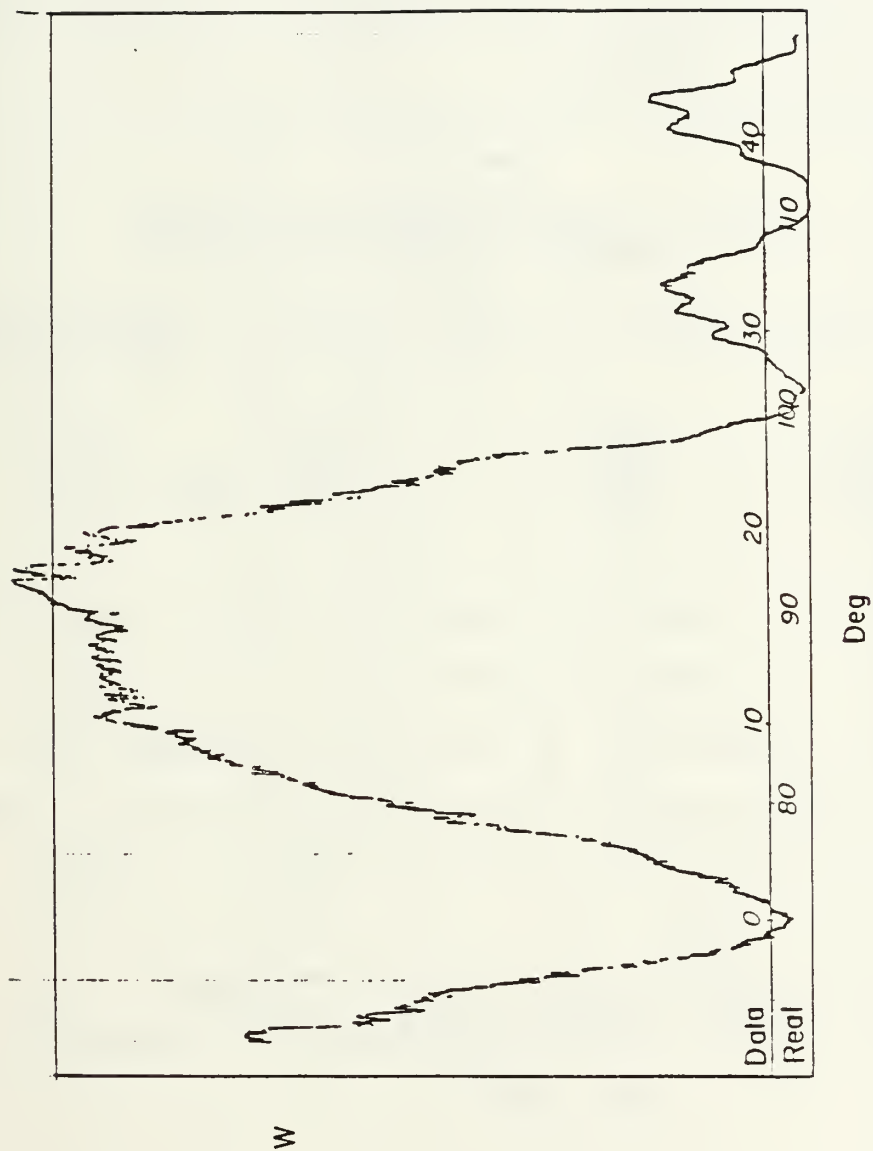


Figure 27 Cerenkov Radiation for the Third Harmonic and where L is Measured at 16.5 cm

The data from Figures 24 through 27 are compared with the theoretical curves in three ways.

1. The data is compared just the way it was collected. There is no angular shift and L used for the theoretical curves from Equation 1 is the measured quantity. Table 3 pertains to this comparison.

TABLE 3
DATA TO THEORY COMPARISON WITH NO
CHANGES IN L OR ANGLE

Data Figure	Compare Figure	L (cm) (measured)	Angular Shift (degrees)
(24)	(28)	14.0	0.0
(25)	(29)	14.0	0.0
(26)	(30)	14.0	0.0
(27)	(31)	16.5	0.0

2. No angular shift is made in the data is made but an effective L is used in Equation (1). The effective L is calculated by measuring the angular width of the major lobes in the data and applying this to the relation in Equation (1) that says the nulls in the diffraction pattern occur when,

$$u = n\pi = \frac{kL}{2} (\cos \theta_c - \cos \theta) \quad (\text{Equation 2})$$

where

$$n = 0, 1, 2, 3, \dots$$

Table (4) pertains to this comparison.

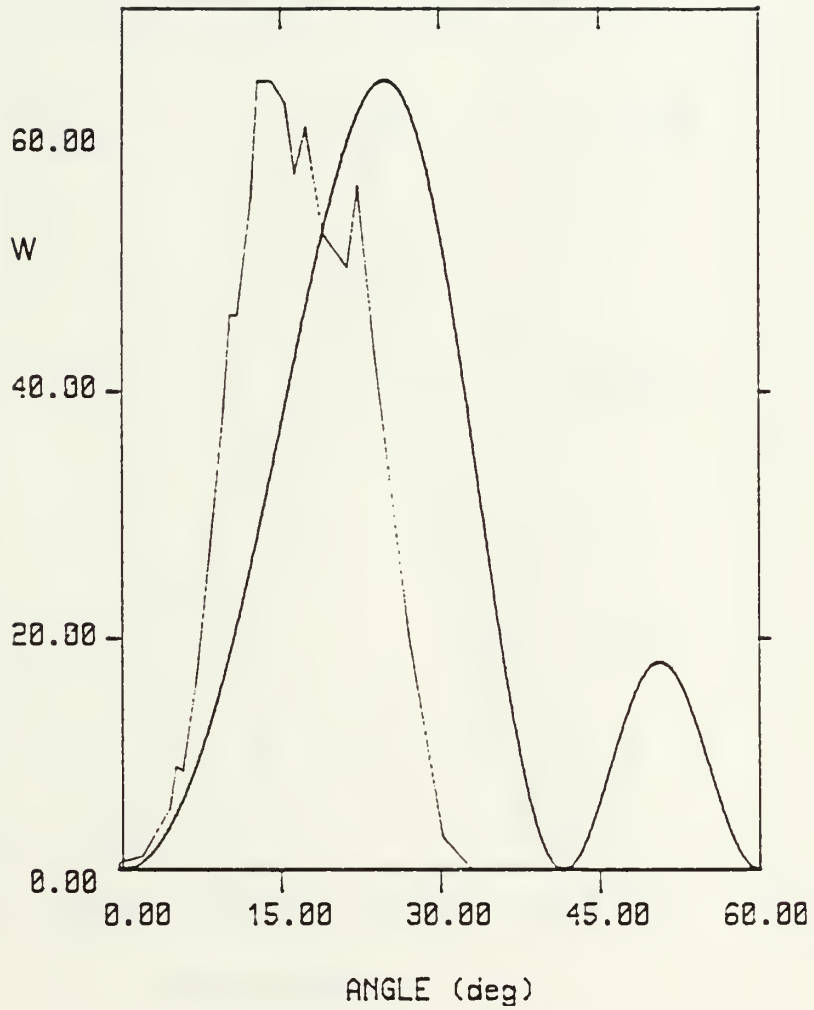


Figure 28 Cerenkov Radiation Data From Figure 24 Compared with Theoretical Curves where $L=14.0$ cm and the Angular Shift is 0.0 Degrees

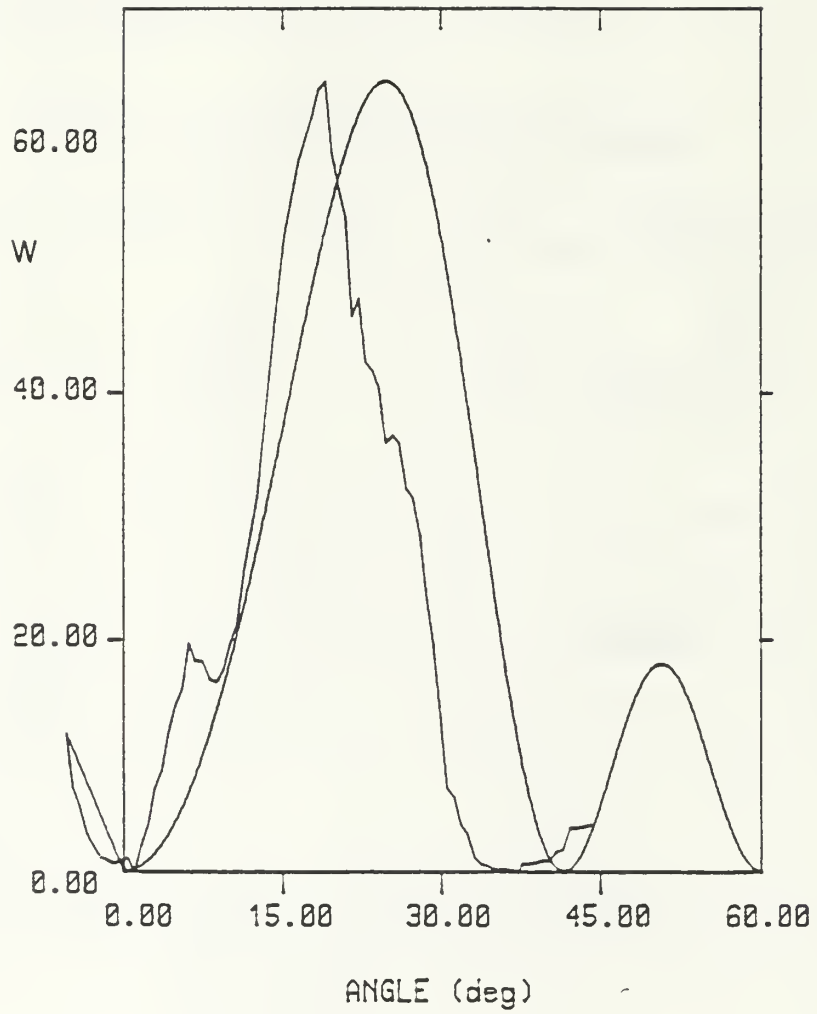


Figure 29 Cerenkov Radiation Data From Figure 25
 Compared with Theoretical Curves where $L=14.0$ cm and
 the Angular Shift is 0.0 Degrees

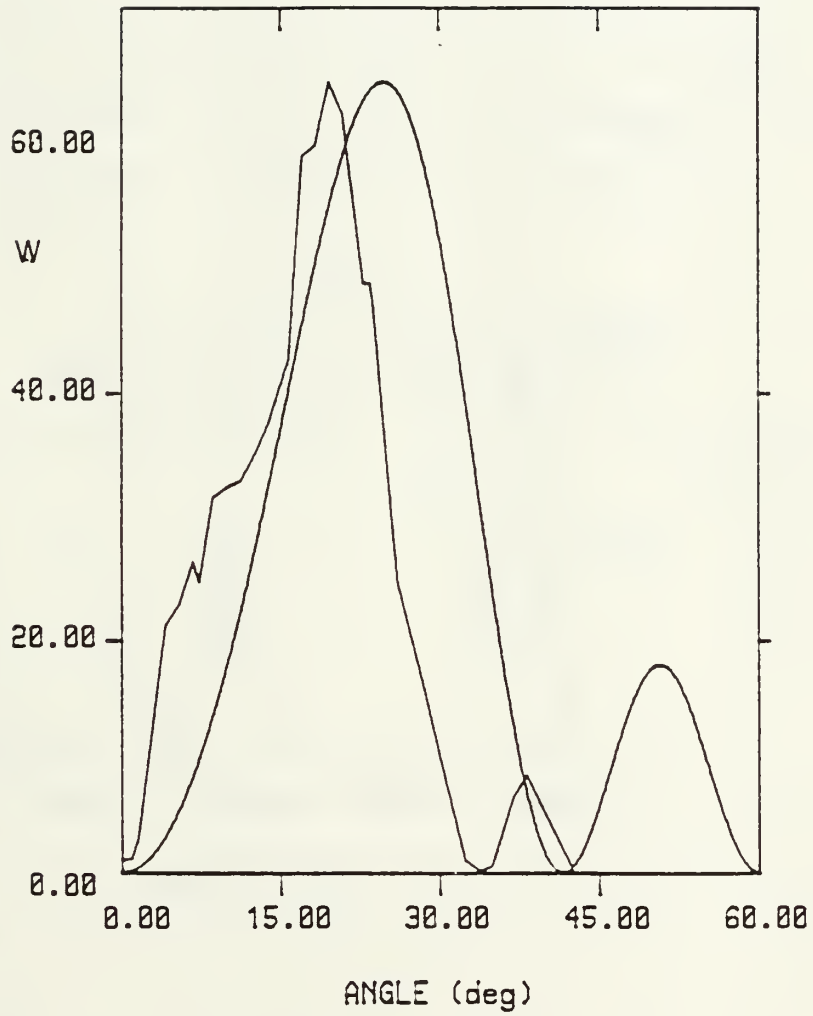


Figure 30 Cerenkov Radiation Data From Figure 26 Compared with Theoretical Curves where $L=14.0$ cm and the Angular Shift is 0.0 Degrees

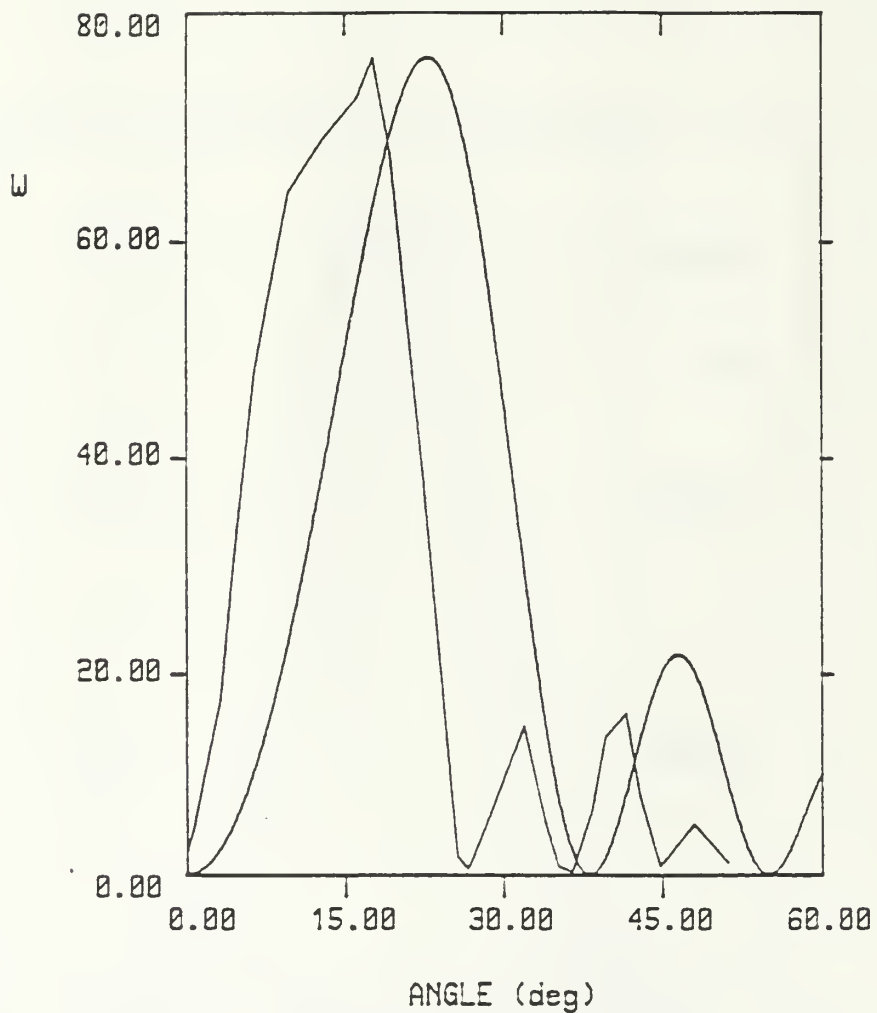


Figure 31 Cerenkov Radiation Data From Figure 27 Compared with Theoretical Curves where L=16.5 cm and the Angular Shift is 0.0 Degrees

TABLE 4

DATA TO THEORY COMPARISON WITH
CALCULATED L BUT NO CHANGE IN ANGLE

Data Figure	Compare Figure	L (cm) (calculated)	Angular Shift (degrees)
(24)	(32)	21.0	0.0
(25)	(33)	16.5	0.0
(26)	(34)	20.0	0.0
(27)	(35)	33.0	0.0

3. The angle in the data is shifted until the peaks of the data and the theory match. The L used is the measured quantity. Table (5) pertains to this comparison.

TABLE 5

DATA TO THEORY COMPARISON WITH
ANGULAR SHIFT BUT NO CHANGE IN L

Data Figure	Compare Figure	L (cm) (measured)	Angular Shift (degrees)
(24)	(36)	14.0	7.0
(25)	(37)	14.0	5.4
(26)	(38)	14.0	8.0
(27)	(39)	16.5	7.5

B. CONCLUSIONS

Experimental verification of Equation 1 is still not absolute. After examining the comparison curves of Figures 28 through 39 it is speculated that much of the mismatch is still the result of noise. However, some of the discrepancy cannot be explained by noise; for example, the experimental-theoretical comparison is closer with the effective L than with the measured L. If the beam is not,

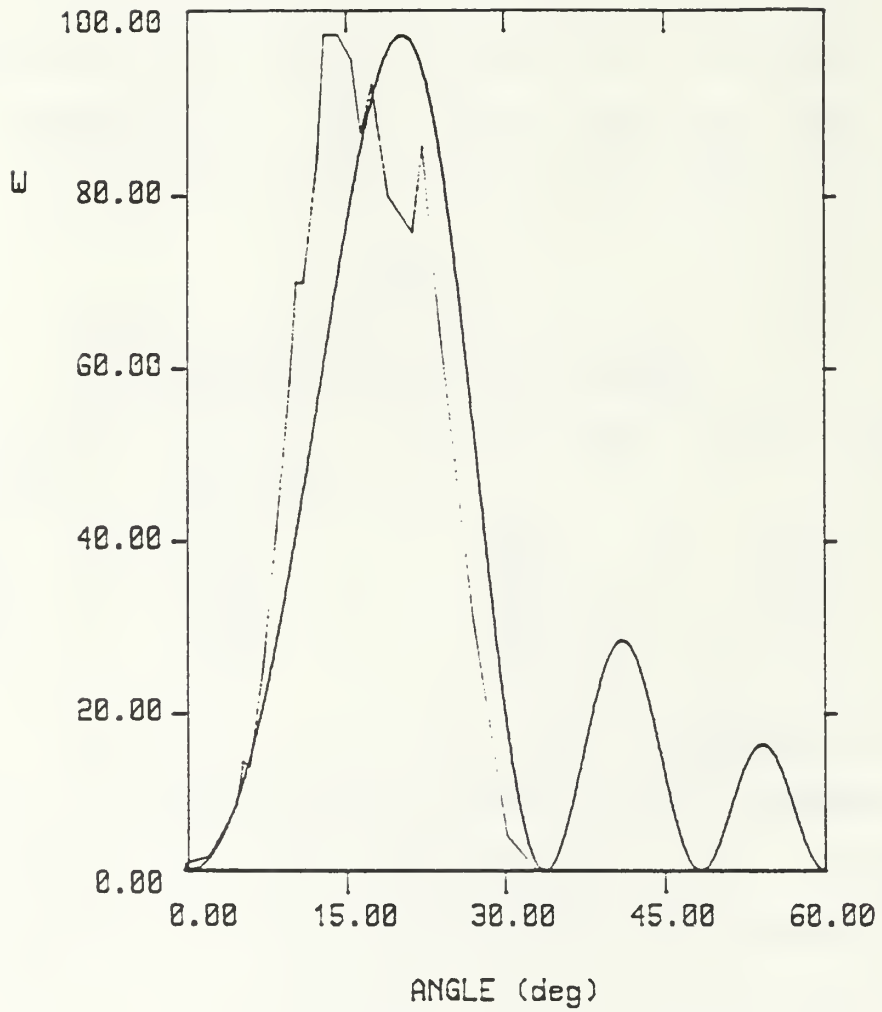


Figure 32 Cerenkov Radiation Data From Figure 24
 Compared with Theoretical Curves where $L=21.0$ cm and
 the Angular Shift is 0.0 Degrees

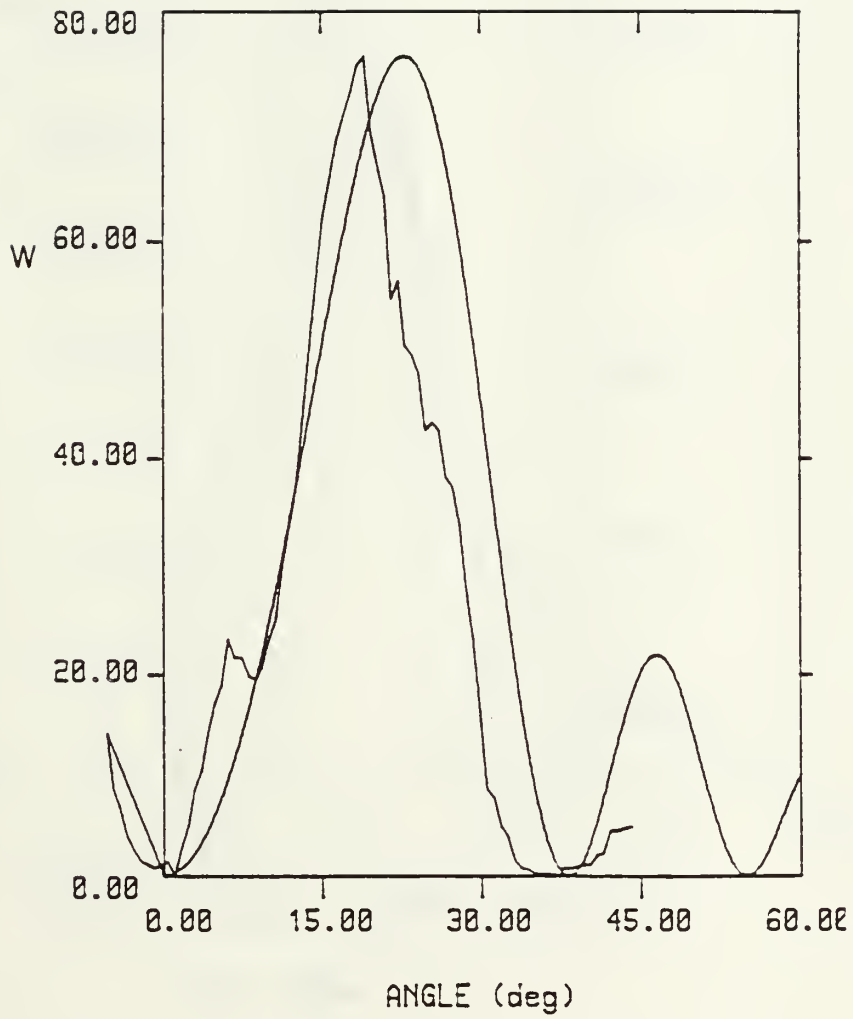


Figure 33 Cerenkov Radiation Data From Figure 25 Compared with Theoretical Curves where $L=16.5$ cm and the Angular Shift is 0.0 Degrees

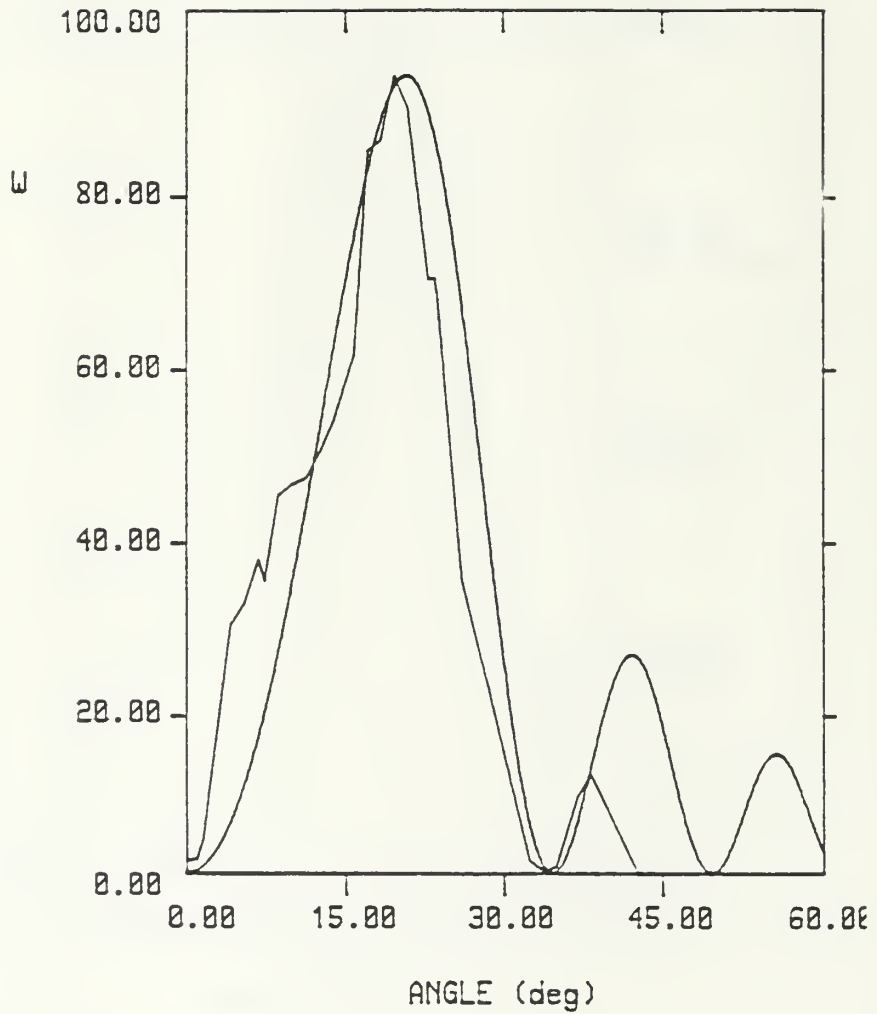


Figure 34 Cerenkov Radiation Data From Figure 26 Compared with Theoretical Curves where L=20.0 cm and the Angular Shift is 0.0 degrees

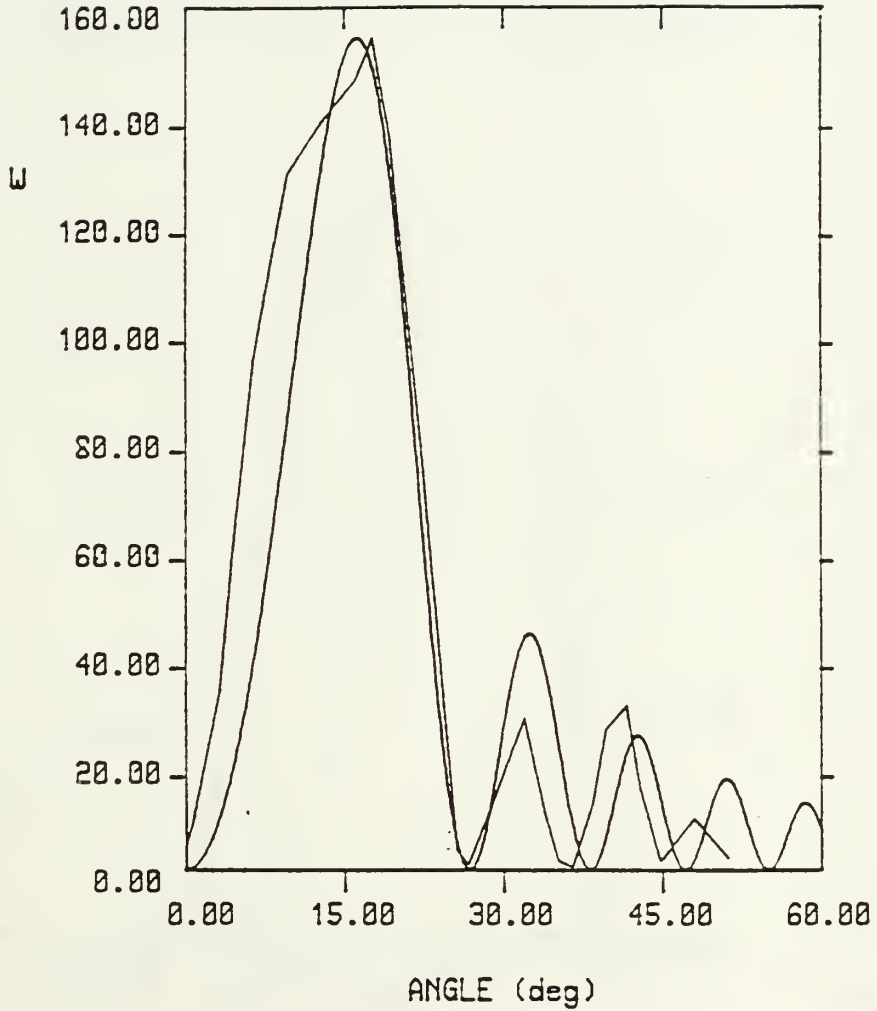


Figure 35 Cerenkov Radiation Data From Figure 27 Compared with Theoretical Curves where $L=33.0$ cm and the Angular Shift is 0.0 Degrees

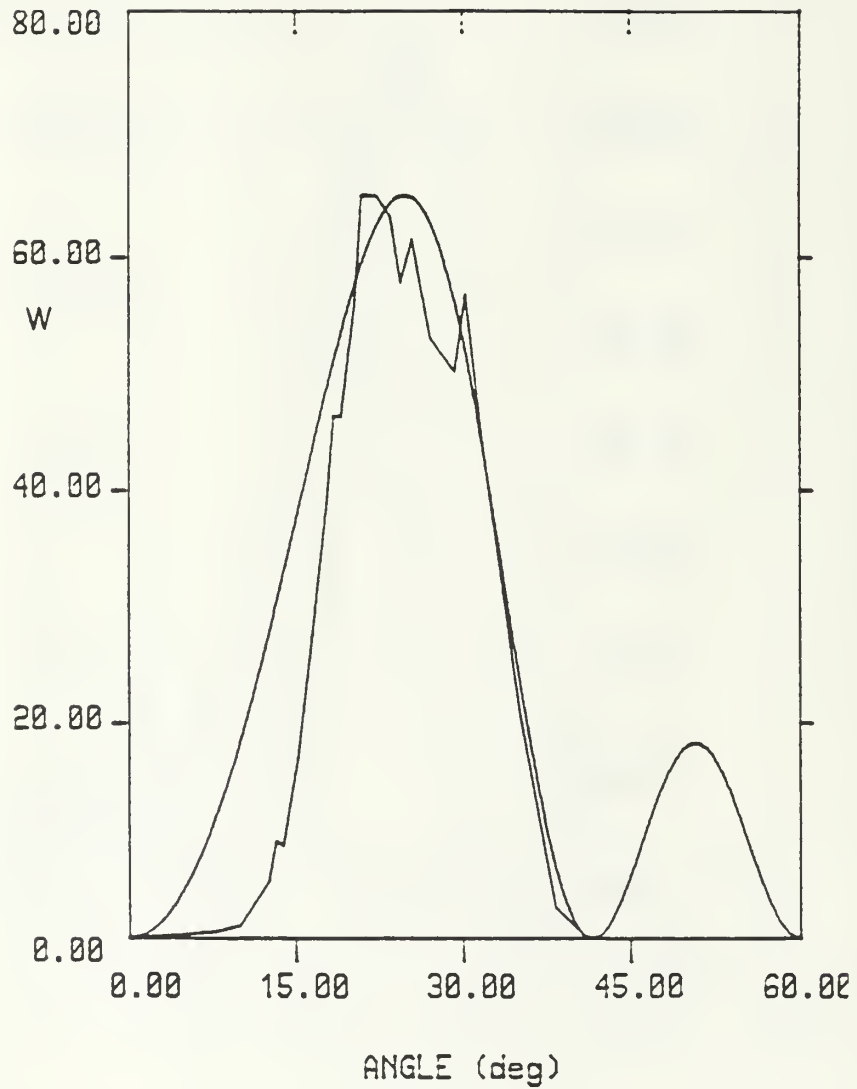


Figure 36 Cerenkov Radiation Data From Figure 24
 Compared with Theoretical Curves where $L=14.0$ cm and
 the Angular Shift is $+7.0$ Degrees

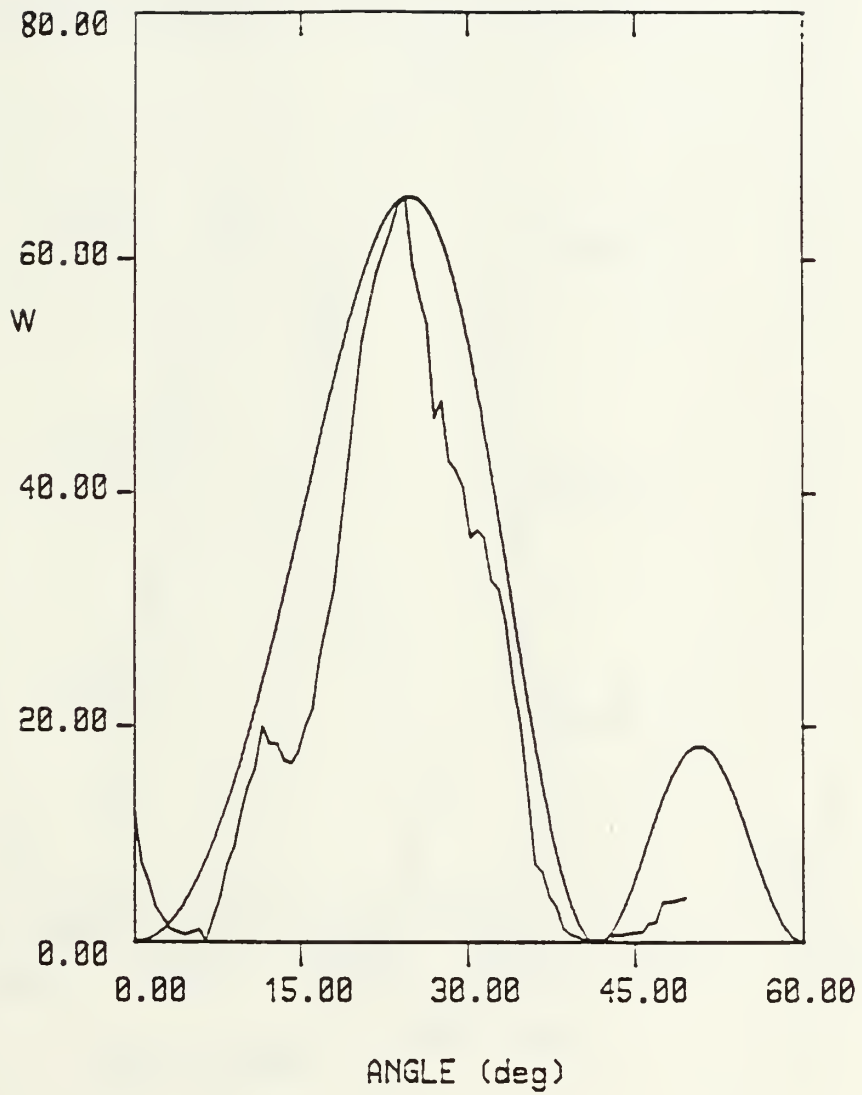


Figure 37 Cerenkov Radiation Data From Figure 25
 Compared with Theoretical Curves where $L=14.0$ cm and
 the Angular Shift is $+5.4$ Degrees

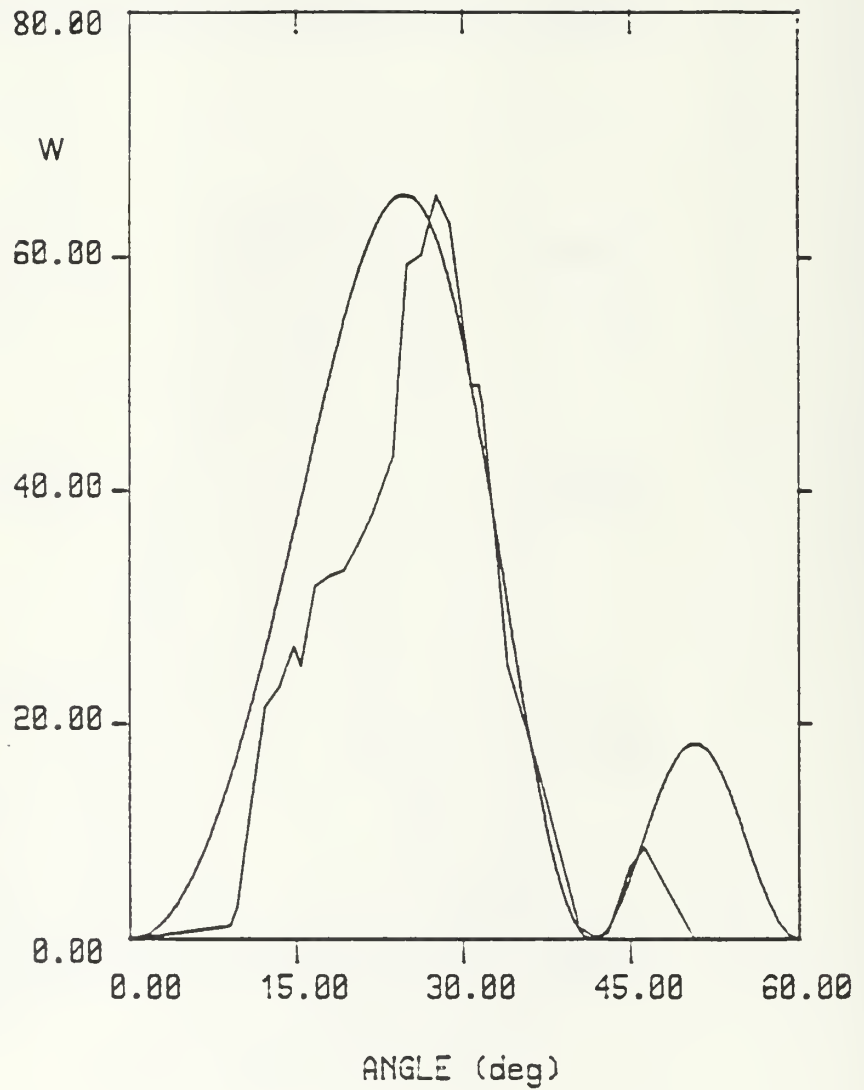


Figure 38 Cerenkov Radiation Data From Figure 26 Compared with Theoretical Curves where $L=14.0$ cm and the Angular Shift is $+8.0$ Degrees

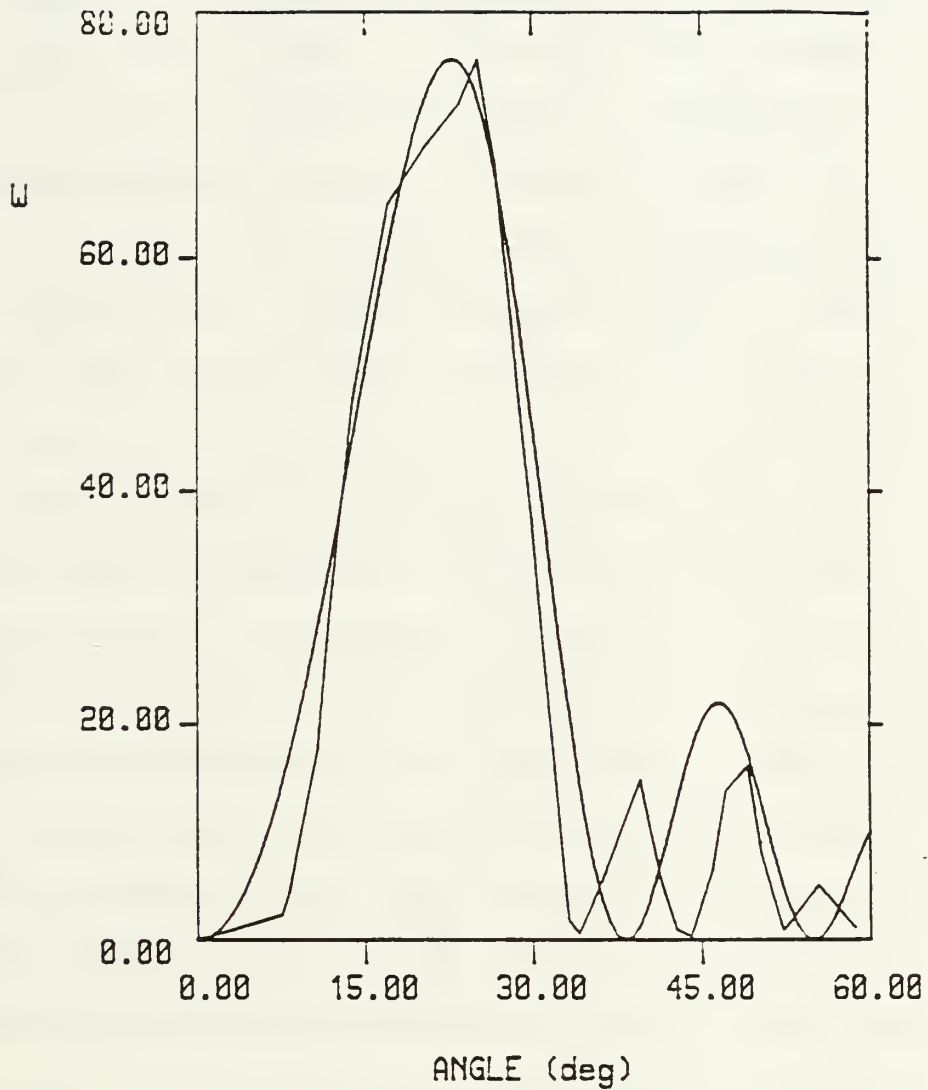


Figure 39 Cerenkov Radiation Data From Figure 27 Compared with Theoretical Curves where $L=16.5$ cm and the Angular Shift is $+7.5$ Degrees

in fact, paraxial but divergent as it passes through air, then fitting the data curves with the theoretical curves requires the use of the "effective L" (Table 4) rather than the measured L. On the other hand, it is conceivable that the angular shift required to match the curves in Table 5 is the uncertainty in the measurement of a) the zero degree point and b) the angle of the null after the peak. It is also to be noted that equation 2 is unable to distinguish between $2L$ and L when a different n is used. We note that L calculated is twice that measured for the case of data Figure 27.

The first lobe in Figures 36 through 39 can be made to fit the curve of Equation 1, concluding, therefore, that the theory is relatively successful in predicting the first lobe. The second lobe from Vujaklija's data (Figure 11) and the present data does not compare successfully with the theory. Consequentially, it is suspected that the experimental arrangement requires improvement. Nonetheless, the suppression of noise allows us to conclude that the fine structure observed in Vujaklija's experiment [Ref. 5] is due to interference effects.

APPENDIX A

DESCRIPTION OF EQUIPMENT

Traveling Dolly - The traveling dolly carries the antenna and the TWT. It travels in an arc around the beam interaction along a wooden, semicircular platform. The dolly is attached to one end of a rigid aluminum tube, of length (r), whose other end is attached to a pivot point directly beneath the mirror (Figure (13)). In this experiment (r) was set at a constant 1.6 meters. The dolly's locomotion is provided by a thirty volt variable speed electric motor remotely operated from the control room. At near full speed the dolly is able to transit a seventy degree arc in eighteen seconds. The dolly is equipped with a ten turn, zero to ten thousand ohm potentiometer for remotely indicating the antenna's position in angle to the beam. The knurl of the potentiometer is replaced with a wheel that rolls on the wooden platform as the dolly moves. The input to the potentiometer is a constant 5 VDC fed from a power supply in the control station. The output varies from near zero voltage to five volts according to the dolly's position in angle to the beam. The output of the potentiometer leads to the X component of the X/Y recorder which is scaled in degrees. Calibration of theta was made and checked with a

chartmaker's three armed protractor.

Mirror - A one foot square aluminum sheet 0.040 inches thick acting as a mirror was placed in the beam path to reflect the Cerenkov radiation toward the antenna. Figure (13) shows the geometry of this setup. Without the mirror it would be impossible to measure Cerenkov at zero angle theta without having the antenna enter the beam path.

Absorbing hood - The absorbing hood consists of a one foot square by three foot long open wooden frame constructed of one inch by one inch lumber. The hood was attached to the rigid pipe between the antenna and the interaction length so that the radiation path to the antenna passed through the hood lengthwise. When covered with microwave absorbing airmat the hood acted as an attenuator, especially to signals not coming from the interaction length.

Beam Cover - A one foot square by six foot long open frame similar to the hood was covered lengthwise with aluminum sheet metal and placed in the beam path down-beam of L. Its purpose was to cover the portion of the beam not to be included as part of L.

Antennas - Two types of microwave antennas are used in this experiment. One is a 2 to 18 GHz pyramidal antenna which attaches directly to coaxial cabling, and the other is an X band 0.01 square meter horn antenna which attaches to a wave guide. A wave guide to coaxial adapter is used with the

horn. At a radius of 1.62 meters from a radiating source the horn covered 0.0043 steradians. The pyramidal antenna was used for experiments in noise reduction while the horn was used for both noise reduction and for mapping Cerenkov radiation.

Wave Guide - A five centimeter section of X band waveguide is inserted between the horn and the waveguide-coaxial adapter. It has a cutoff frequency of 6.6 GHz and, therefore, serves the purpose of eliminating signals in the fundamental frequency and the second harmonic. Figure (14) shows the characteristics of this particular section. It is noted that at the third harmonic the loss is less than 0.5 dB whereas for frequencies less than 6.6 GHz the loss is greater than 30 dB. The reference line is at 0.0 dB. These graphs were obtained using the HP Scalar Analyzer available at the Electrical Engineering Department Microwave Laboratory at the Naval Postgraduate School.

Coaxial Cable (RG 9/U) - Two lengths, totalling 2.7 meters, are used in the experiment. Cabling is kept to a minimum as it adds about 1.45 dB per meter loss to the signal train at the third harmonic frequency. Figure (15) shows the characteristics for the 2.7 meter length from 7 to 12 GHz. Note in the figure, the cursor on the left is at 8.56 GHz while the one on the right (slightly lower) is at 11.42 GHz.

Travelling Wave Tube Amplifier (WJ-276-2) - The TWT used in this experiment has approximately 25 dB of gain through a frequency range from 7 to 11 GHz. Figure (16) shows the characteristics of the signal train through the wave guide, the adapter, the cabling, and the TWT. At 8.5 GHz the gain is 21.96 dB. Note the 6.2 dB difference between the gain at 8.5 GHz and 11.4 GHz.

Crystal Detector (HP 420A) - The crystal detector used in this experiment had the purpose of demodulating the Cerenkov pulse to form a 60 Hz pulse envelope visible to the oscilloscope and to the IC network.

Ortec 450 Research Amplifier - The experimental amplifier amplified the relatively weak pulse (millivolts) coming from the crystal detector to the 0 to 5 volt range necessary to be utilized by the IC network.

High Speed Sample and Hold Network (SHM 20C IC) - When the HSSHN is triggered by the linac 60 Hz trigger it samples the voltage of the Cerenkov pulse from the research amplifier and holds it until the next trigger. The trigger is adjusted in time so that the sample is taken as close to the peak of the Cerenkov pulse as possible. Therefore, the output, connected to the Y component of the XY recorder, is a steady 0 to 5 volts, updated every 16 milliseconds, representing the magnitude of Cerenkov radiation at a given angle. Figure (17) is the circuit diagram of the network and

Figure (18) illustrates Cerenkov signal morphology from the beam to the XY recorder.

Tunable YIG Filter (IM IMF 1800)- The YIG filter is tunable over a range from 1 to 18 GHz with a 8 dB insertion loss. In this experiment, a cable was fabricated so that the filter head could be placed in the experiment room while the tuner was placed in the control room.

Band Pass Filter (PMI Model 1085A)- This lossless filter with a bandpass from 8 to 10 GHz could be inserted right after the antenna to filter out all but the third harmonic.

APPENDIX B

SUGGESTIONS FOR FUTURE WORK

1. Acquire a lossless band pass filter which is now available from the Microwave Laboratory.
2. Move the experimental amplifier from the control room to the experiment station. This suggestion would result in virtually eliminating all of the cabling noise.
3. Acquire more of the blue spongy absorber material and shield the experiment room extensively.
4. Design a precisely adjustable mirror stand so that L and the mirror angle can be accurately defined.

APPENDIX C

TABULATION OF DATA

The following tables contain the values tabulated from the data in Figures 24 through 27. These values were used to develop the plots in Figures 28 through 39.

TABLE 6

Tabulated Data From Figure 24

Data Angle (degree)	W (Normalized to theoretical peak)
-11.50	38.00
-10.90	36.00
-9.60	28.00
-9.00	24.00
-8.30	14.00
-7.40	9.00
-6.40	7.00
-5.80	4.00
-4.50	1.00
-3.20	1.00
-2.60	1.20
-1.90	1.00
0.60	0.60
0.00	0.60
1.30	1.00
2.60	1.20
3.20	1.50
4.50	3.00
5.10	5.00
5.80	5.00
6.40	7.50

TABLE 6 (Cont'd.)

7.70	9.50
8.30	14.00
9.00	17.00
10.30	24.00
10.90	24.00
11.50	28.50
12.20	29.00
12.90	34.00
14.10	34.50
14.70	34.00
15.40	32.50
16.00	31.00
16.70	30.00
17.30	32.00
17.90	29.00
18.60	29.00
19.20	28.50
19.90	27.50
20.50	28.00
21.20	26.00
22.10	29.00
23.10	24.00
23.70	22.50
25.60	15.00
27.20	8.00
28.20	4.00
28.80	3.00
30.10	1.60
31.40	1.00
32.00	0.80
32.70	0.30

TABLE 7

Tabulated Data from Figure 25

Data Angle (degree)	W (Normalized to theoretical peak)
-9.60	53.50
-8.90	53.00
-8.00	40.00
-6.40	21.00
-4.80	9.00
-3.80	4.00
-3.50	4.00
-2.90	2.50
-2.20	1.60
-1.30	1.00
-0.60	0.80
0.00	0.70
0.60	1.10
1.30	1.00
1.90	1.50
2.50	2.00
3.80	6.00
4.50	7.50
5.10	10.00
6.70	13.00
8.00	12.00
9.30	11.00
11.20	14.00
11.90	18.00
12.80	20.00
13.80	24.00
14.40	29.00
15.40	34.00
16.30	38.00
17.60	41.00
18.30	42.00
18.90	44.00
19.60	44.50
20.80	38.00
22.10	31.00
22.40	33.00
24.00	28.00
25.30	24.00
26.00	24.50

TABLE 7 (Cont'd.)

26.60	24.00
27.20	21.50
28.50	19.00
29.80	14.00
30.40	9.00
31.10	5.00
31.70	5.00
33.00	2.50
33.70	1.00
35.30	0.00
38.50	0.50
40.10	1.00
41.70	1.50
42.90	3.00
44.90	3.20

TABLE 8

Tabulated Data from Figure 26

Data Angle (degree)	W (Normalized to theoretical peak)
0.00	1.00
0.64	1.00
1.60	2.00
2.50	5.50
3.50	12.00
5.10	14.00
5.70	15.00
6.70	14.10
8.30	19.00
10.80	19.50
12.80	21.50
14.70	24.00
15.70	29.00
16.34	34.00
17.60	35.00
18.90	38.00
20.19	36.00
21.50	32.00
22.40	28.00
23.00	28.00
25.00	19.00
25.90	12.00
27.60	9.00
30.10	3.50
32.40	0.50
33.30	0.00
33.60	0.20
35.60	1.30
36.53	4.20
37.80	5.00
41.70	0.60

TABLE 2

Tabulated Data from Figure 27

Data Angle (degree)	W (Normalized to theoretical peak)
0.00	0.00
0.60	2.00
1.20	4.00
1.90	6.00
2.50	10.00
3.20	12.00
3.80	15.00
4.50	22.00
4.80	28.00
5.10	25.00
5.70	30.00
6.40	36.50
7.00	39.00
7.70	42.00
8.30	47.00
9.60	50.00
10.20	55.00
10.60	50.00
11.50	53.00
12.80	54.00
15.40	56.00
17.30	61.00
19.80	52.00
22.40	27.00
24.30	7.00
24.90	2.00
26.60	-1.00
32.00	10.00
35.20	-1.00
36.20	-1.50
38.40	4.00
39.70	10.00
41.60	11.00
44.80	-1.00
48.70	3.00
51.90	0.00

LIST OF REFERENCES

1. Jelley, J. V., Cerenkov Radiation and Its Applications, Pergamon Press, 1958.
2. Buskirk, F. R. and Neighbours, J. R., "Cerenkov Radiation From Periodic Electron Bunches," *Physical Review A*, Volume 28, Number 3, September, 1983.
3. Buskirk, F. R. and Neighbours, J. R., Naval Postgraduate School, Report Number NPS-61-83-010, "Diffraction Effects in Cerenkov Radiation," June 1983.
4. Turner, E. R., "Form Factor Effects on Microwave Cerenkov Radiation," Master's Thesis, Naval Postgraduate School, Monterey, 1984.
5. Vujaklija, M., "Cerenkov Radiation from Periodic Electron Bunches for Finite Emission Length in Air," Master's Thesis, Naval Postgraduate School, Monterey, 1984.
6. Skolnik, M. I., Introduction to Radar Systems, p. 229, McGraw-Hill, 1980.
7. Saglam, Ahmet, "Cerenkov Radiation," Master's Thesis Naval Postgraduate School, Monterey, 1982.
8. Buskirk, F. R. and Neighbours, J. R., "Cerenkov Radiation From a Finite-Length Path in a Gas," *Physical Review A*, Volume 29, Number 6, June, 1984.
9. Newton, Lawrence A., "Cerenkov Radiation Generated by Periodic Electron Bunches in a Finite Air Path," Master's Thesis, Naval Postgraduate School, Monterey, 1983.

INITIAL DISTRIBUTION LIST

	No. Copies
1. Library, Code 0142 Naval Postgraduate School Monterey, California 93943-5100	2
2. Physics Library, Code 61 Department of Physics Naval Postgraduate School Monterey, California 93943-5100	2
3. Professor J. R. Neighbours, Code 61Nb Department of Physics Naval Postgraduate School Monterey, California 93943-5100	5
4. Professor X. K. Maruyama B108, Bldg. 245 National Bureau of Standards Gaithersburg, Maryland 20899	5
5. Professor F. R. Buskirk, Code 61Bs Department of Physics Naval Postgraduate Monterey, California 93943-5100	2
6. CDR Robert G. Bruce OP 375 OPNAV Support Activity Washington D.C. 20350	2
7. Defense Technical Information Center Cameron Station Alexandria, Virginia 22304-6145	2

214078

Thesis

B8247 Bruce

c.1 Cerenkov radiation
from periodic bunches
for a finite beam path
in air.

3 JUN 86
16 NOV 87

33162
33326

214078

Thesis

B8247 Bruce

c.1 Cerenkov radiation
from periodic bunches
for a finite beam path
in air.



thesB8247

Cerenkov radiation from periodic bunches



3 2768 000 62595 8
DUDLEY KNOX LIBRARY